

# outline

- Giant Magnetoresistance, Tunneling Magnetoresistance
- Spin Transfer Torque
- Pure Spin current (no net charge current)
  - Spin Hall, Inverse Spin Hall effects
  - Spin Pumping effect
  - Spin Seebeck effect
- Micro and nano Magnetics

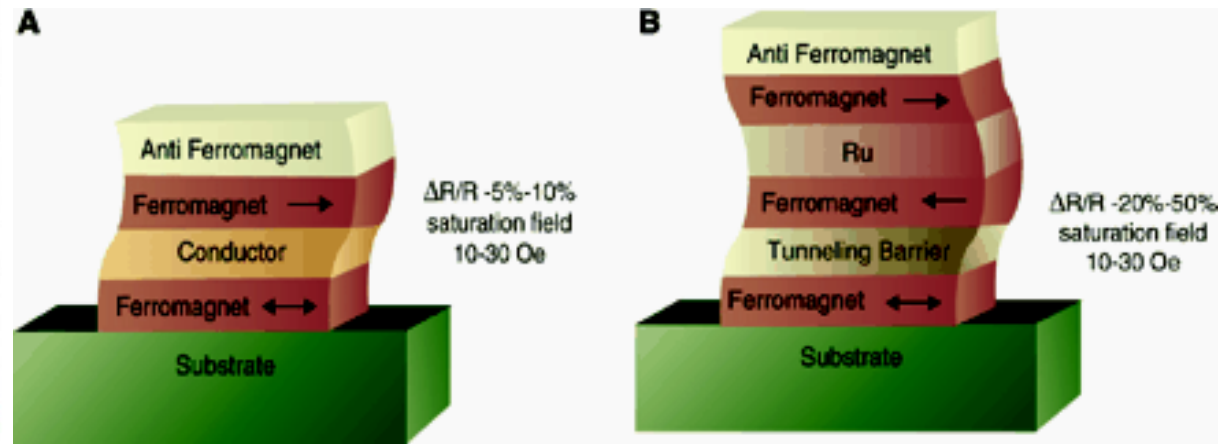
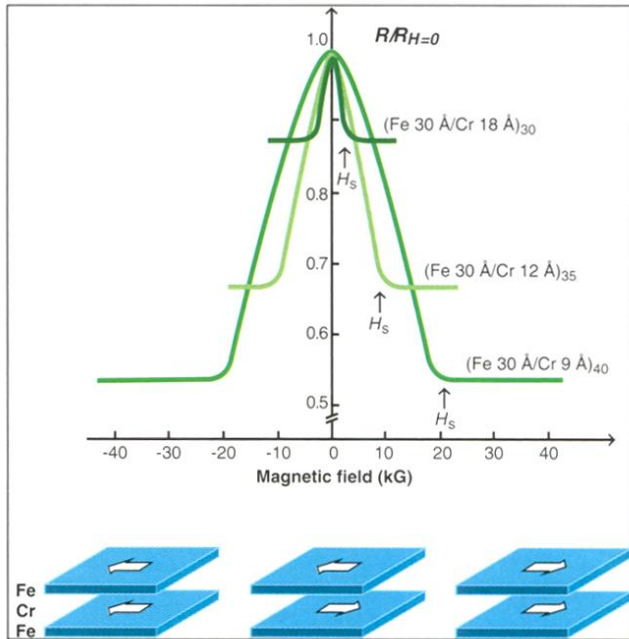
# 2007 Nobel prize in Physics



2007年諾貝爾物理獎得主 左 亞伯·費爾(Albert Fert) 與  
右彼得·葛倫貝格(Peter Grünberg)

(圖片資料來源：Copyright © Nobel Web AB 2007/ Photo: Hans Mehlin)

# Giant Magnetoresistance Tunneling Magnetoresistance



Discovery of Giant MR --  
Two-current model combines  
with magnetic coupling in  
multilayers

Spin-dependent transport structures. (A)  
Spin valve. (B) Magnetic tunnel junction.  
(from Science)

Moodera's group, PRL **74**, 3273 (1995)

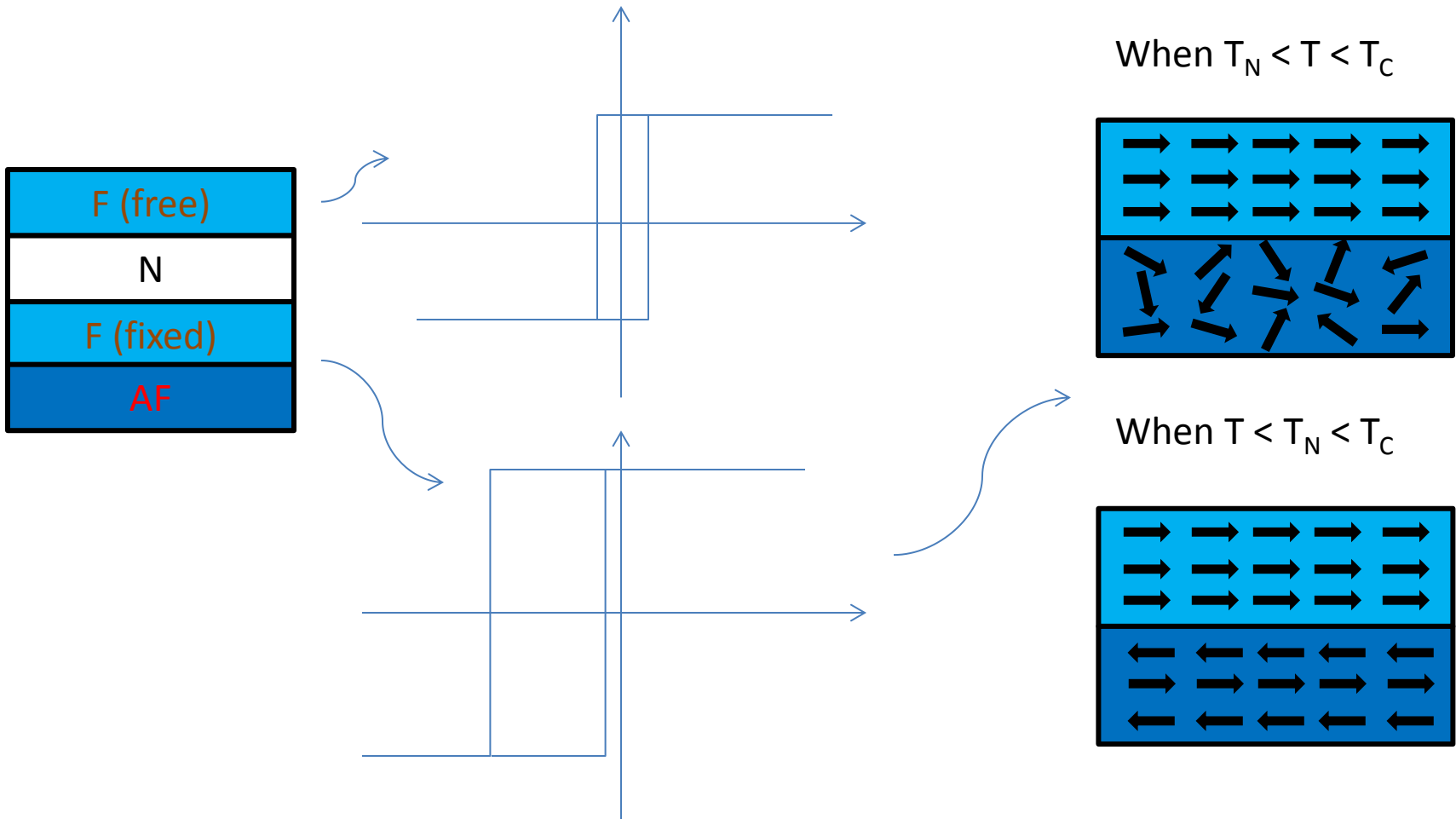
Fert's group, PRL **61**, 2472 (1988)

Miyazaki's group, JMMM **139**, L231(1995)

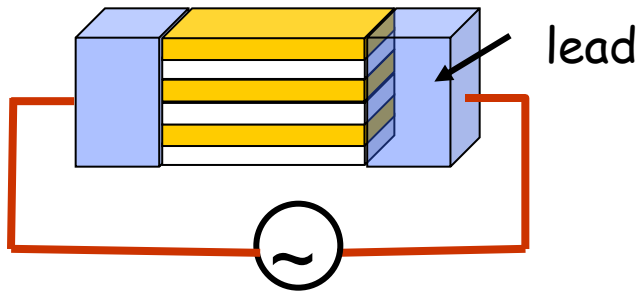
# Spin valve –

a sandwich structure

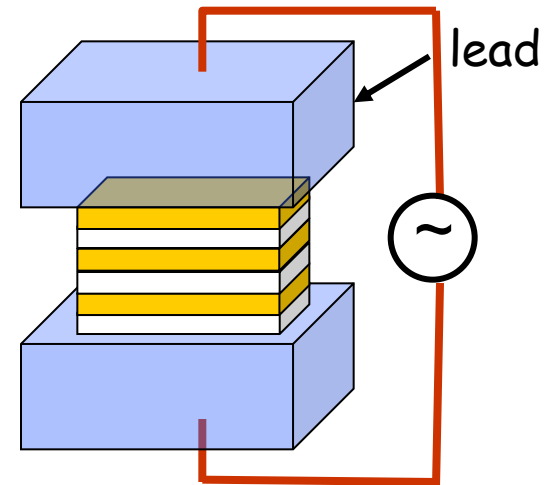
with a free ferromagnetic layer (F) and a fixed F layer  
pinned by an antiferromagnetic (AF) layer



# Transport geometry



CIP geometry



CPP geometry

- In metallic multilayers, CIP resistance can be measured easily, CPP resistance needs special techniques.
- From CPP resistance in metallic multilayers, one can measure interface resistances, spin diffusion lengths, and polarization in ferromagnetic materials, etc.
- CPP magnetoresistance of magnetic multilayers: A critical review  
Jack Bass

Journal of Magnetism and Magnetic Materials 408 (2016) 244–320

# Valet and Fert model of (CPP-)GMR

Based on the Boltzmann equation

A semi-classical model with spin taken into consideration

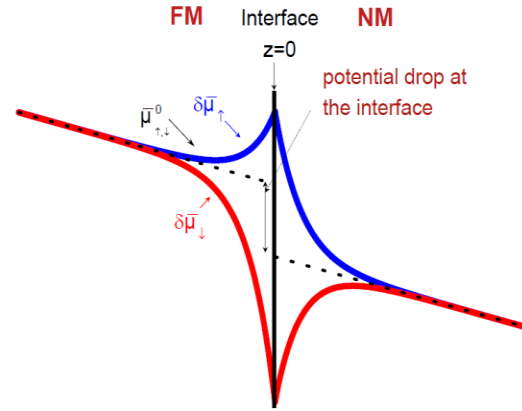
$$j_{+(-)} = \frac{1}{e\rho_{+(-)}} \frac{\partial \mu_{+(-)}}{\partial x}$$

$$j_+ + j_- = j_e$$

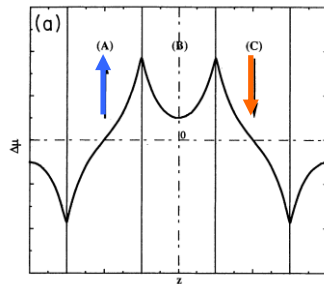
$$\frac{\partial(j_+ - j_-)}{\partial x} = \frac{2eN(E_F)\Delta\mu}{\tau_{sf}}$$

$$\frac{\partial^2 \mu_{+(-)}}{\partial z^2} = \frac{\mu_{+(-)}}{l_{sf}^2}$$

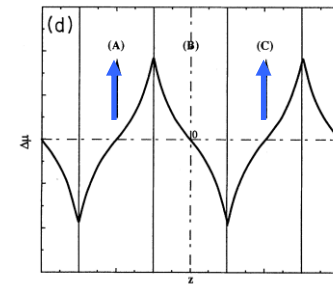
$$l_{sf}^F = \left[ \lambda_{sf}^F / 3(\lambda_{\uparrow}^{-1} + \lambda_{\downarrow}^{-1}) \right]^{1/2}, \quad l_{sf}^N = \left[ \lambda_{sf}^N \lambda / 6 \right]^{1/2}$$



$\Delta\mu$  for antiparallel aligned multilayers

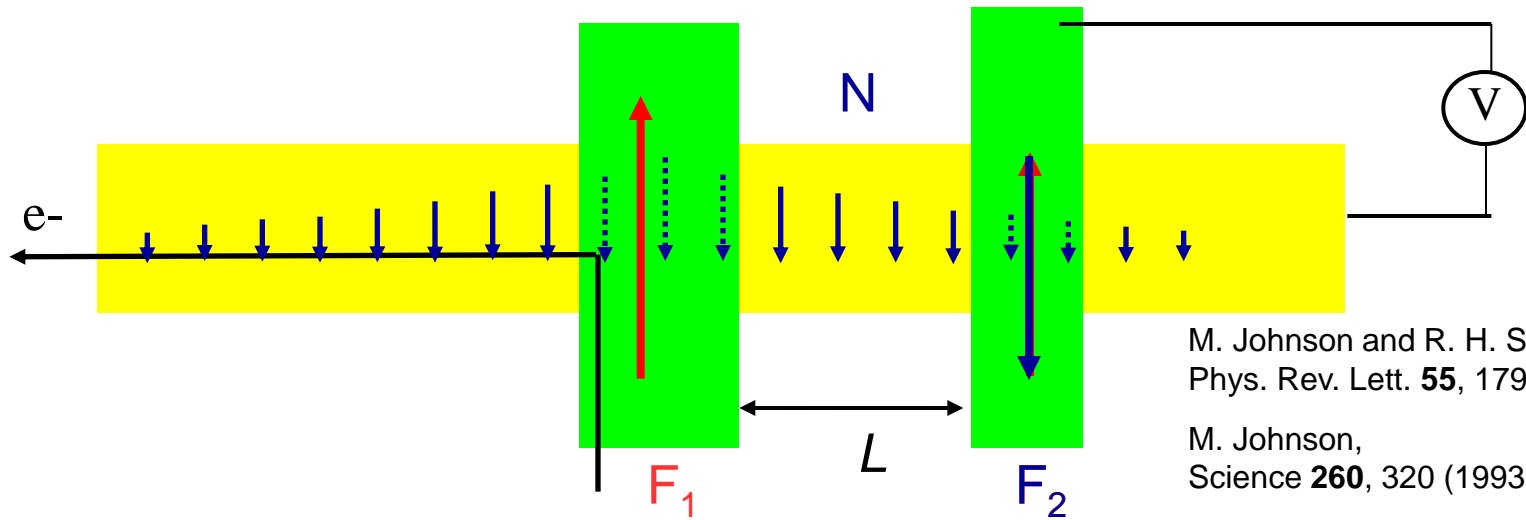


$\Delta\mu$  for parallel aligned multilayers



Spin imbalance induced charge accumulation at the interface is important  
Spin diffusion length, instead of mean free path, is the dominant physical length scale

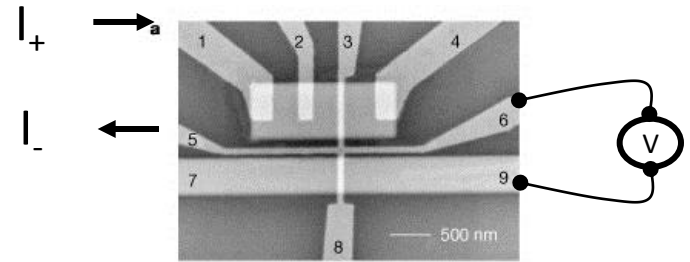
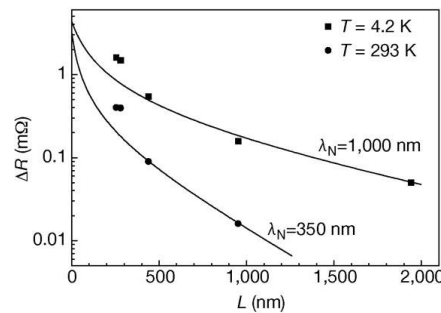
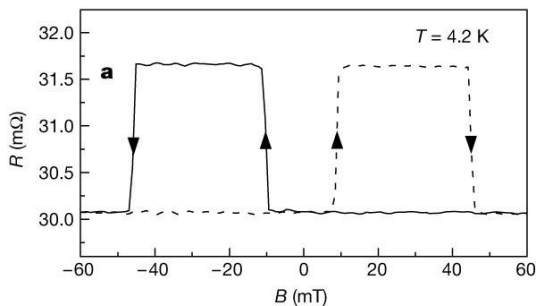
# Spin Diffusion: The Johnson Transistor non-local measurement



M. Johnson and R. H. Silsbee,  
Phys. Rev. Lett. **55**, 1790 (1985)

M. Johnson,  
Science **260**, 320 (1993)

## First Experimental Demonstrations



Cu film:  $\lambda_s = 1 \mu\text{m}$  (4.2 K)

Jedema *et al.*, Nature **410**, 345 (2001)

# outline

- Giant Magnetoresistance, Tunneling Magnetoresistance
- Spin Transfer Torque
- Pure Spin current (no net charge current)
  - Spin Hall, Inverse Spin Hall effects
  - Spin Pumping effect
  - Spin Seebeck effect
- Micro and nano Magnetics



# Spin Transfer Torque

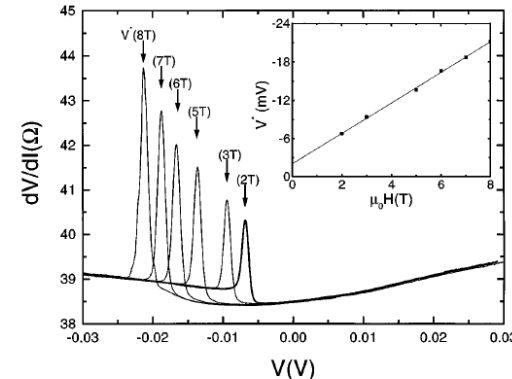
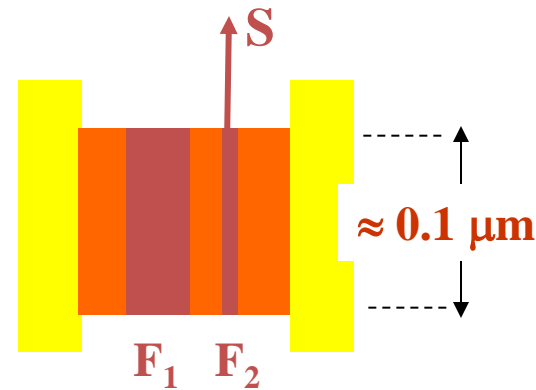
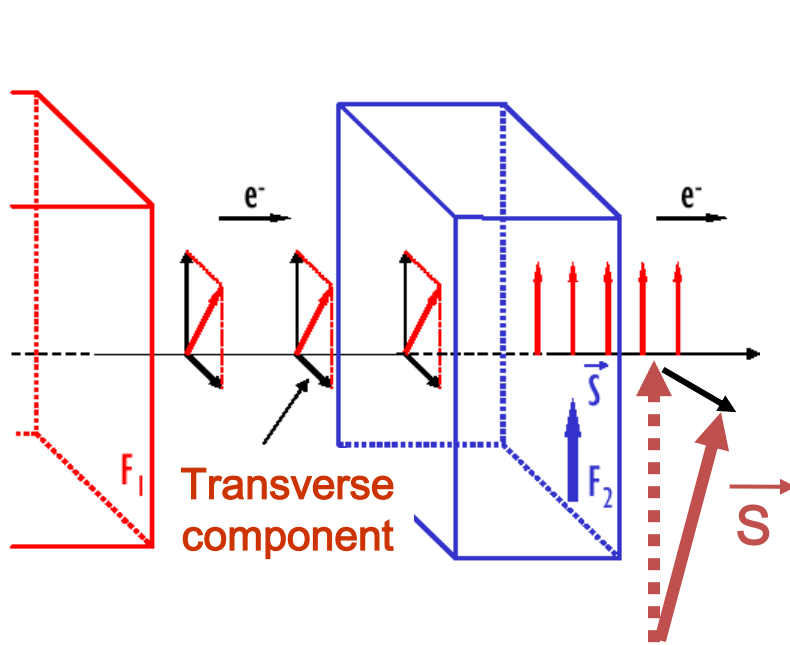


FIG. 1. The point contact  $dV/dI(V)$  spectra for a series of magnetic fields (2, 3, 5, 6, 7, and 8 T) revealing an upward step and a corresponding peak in  $dV/dI$  at a certain negative bias voltage  $V^*(H)$ . The inset shows that  $V^*(H)$  increases linearly with the applied magnetic field  $H$ .

Tsoi et al. PRL **61**, 2472 (1998)

The transverse spin component is lost by the conduction electrons, transferred to the global spin of the layer  $\vec{S}$

$$\dot{\vec{S}}_{1,2} = (I_c g/e) \hat{s}_{1,2} \times (\hat{s}_1 \times \hat{s}_2)$$

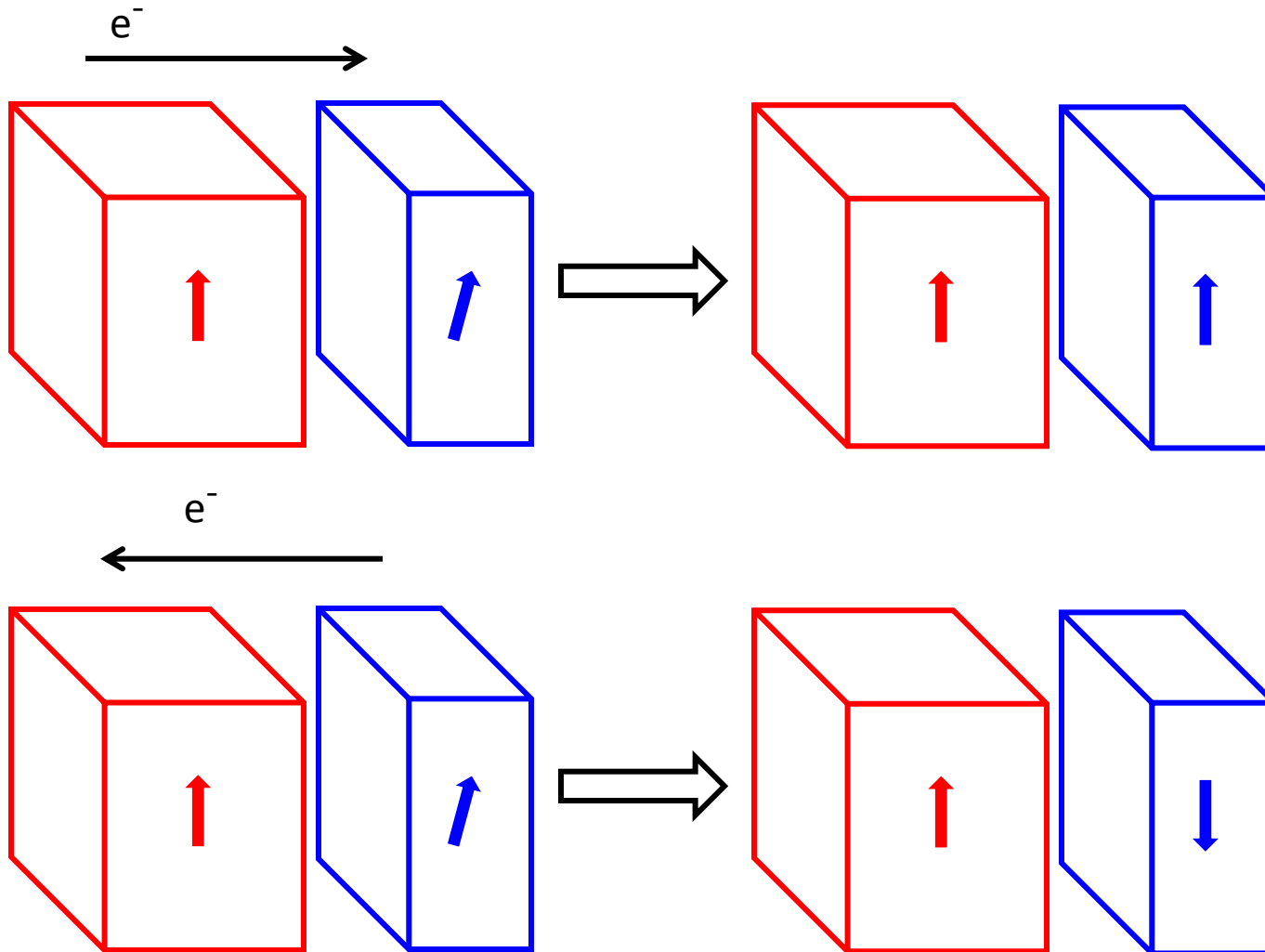
Slonczewski JMMM **159**, L1 (1996)

Modified Landau-Lifshitz-Gilbert (LLG) equation

$$\frac{dm}{dt} = -\gamma m \times H_{eff} + \alpha m \times \frac{dm}{dt} + \frac{\gamma \hbar P I}{2e\mu_0 M_S V} (m \times \sigma \times m)$$

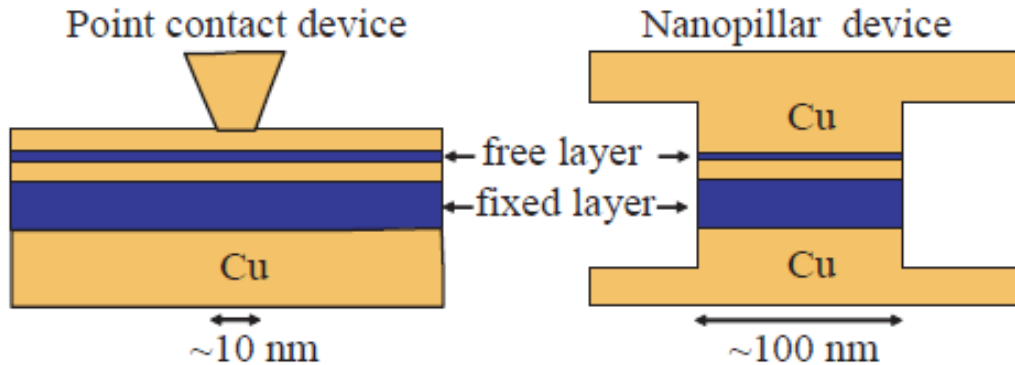
Experimentally determined current density  $\sim 10^{10}$ - $10^{12}$  A/m<sup>2</sup>

# Spin Transfer Torque

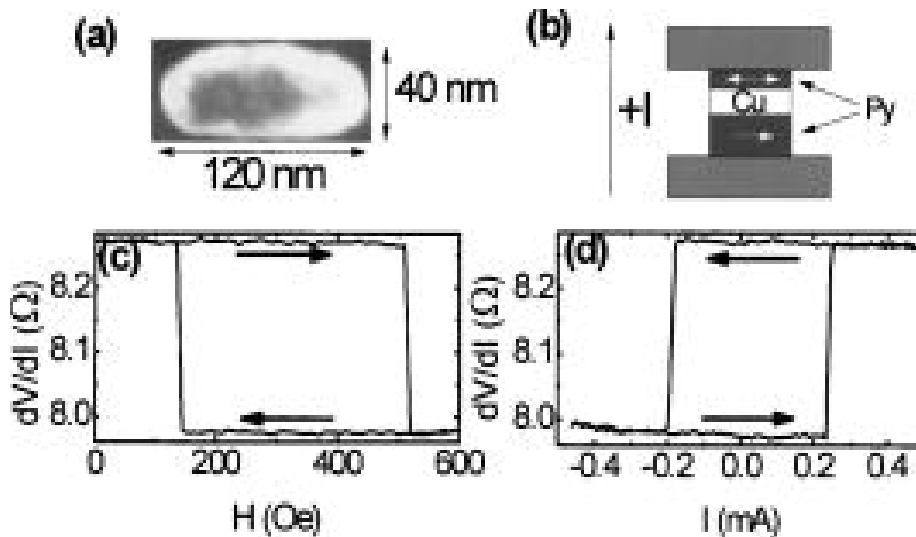


In a trilayer, current direction determines the relative orientation of  $F_1$  and  $F_2$

# Spin Transfer Torque



Ralph and Stiles "[Spin transfer torques](#)". *JMMM* **320**, 1190–1216 (2008).



(c) Minor loop of free layer and (d) spin transfer curve at 293K  
120 Cu/20 Py/12 Cu/X Py/2 Cu/30 Au

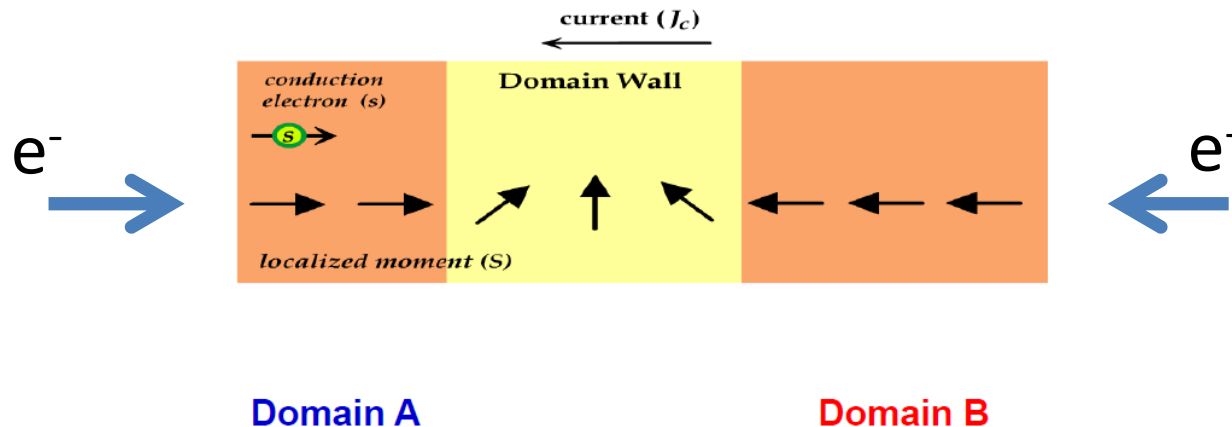
Ralph and Buhrman's group, APL **87**, 112507 (2005)

# Spin Transfer Torque

## Landau-Lifshitz-Gilbert equation with Spin Transfer Torque terms

Current induced domain wall motion

Passing spin polarized current from Domain A to Domain B  $\Rightarrow$  B switches



$$\frac{\partial \vec{M}}{\partial t} = -\gamma \vec{M} \times \vec{H}_{eff} + \frac{\alpha}{M_S} \vec{M} \times \frac{\partial \vec{M}}{\partial t} + \vec{T}_{STT}$$

Berger, *JAP* **55**, 1954 (1984)

Tatara *et. al.*, *PRL* **92**, 086601 (2004)

Zhang *et. al.*, *PRL* **93**, 127204 (2004)

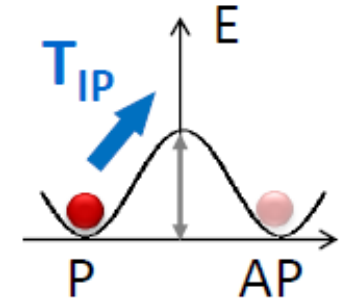
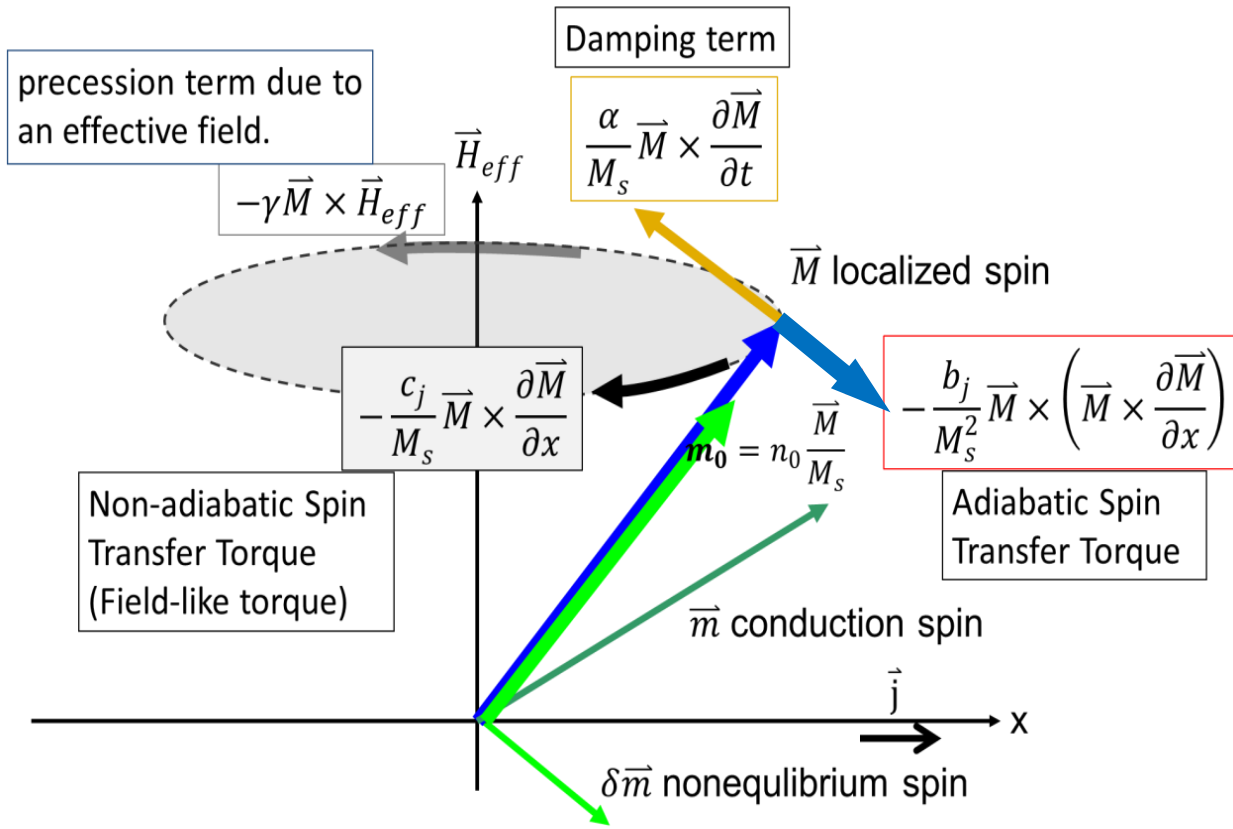
Thiaville *et. al.*, *Europhys. Lett.* **69**, 990 (2005)

Stiles *et. al.*, *PRB* **75**, 214423 (2007)

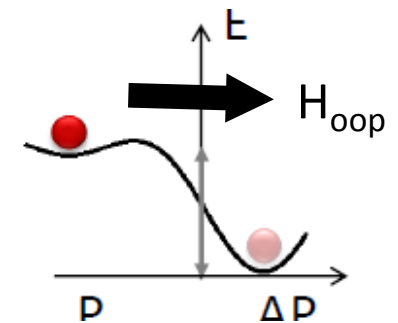
# Spin Transfer Torque

Landau-Lifshitz-Gilbert equation with Spin Transfer Torque terms

$$\frac{\partial \vec{M}}{\partial t} = \underbrace{-\gamma \vec{M} \times \vec{H}_{\text{eff}}}_{\text{precession term due to an effective field.}} + \underbrace{\frac{\alpha}{M_s} \vec{M} \times \frac{\partial \vec{M}}{\partial t}}_{\text{Damping term}} - \underbrace{\frac{b_j}{M_s^2} \vec{M} \times (\vec{M} \times \frac{\partial \vec{M}}{\partial x})}_{\text{Adiabatic Spin Transfer Torque}} - \underbrace{\frac{c_j}{M_s} \vec{M} \times \frac{\partial \vec{M}}{\partial x}}_{\text{Non-adiabatic Spin Transfer Torque (Field-like torque)}} \quad b_j, c_j \sim JP/t$$



In-plane torque  
Anti-damping  
Destabilizes M



Out-of-plane torque  
Field-like torque  
Modifies energy barrier

# Onsager reciprocity relations

Conjugate variables

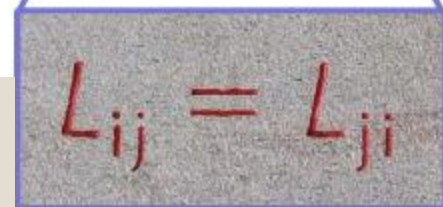
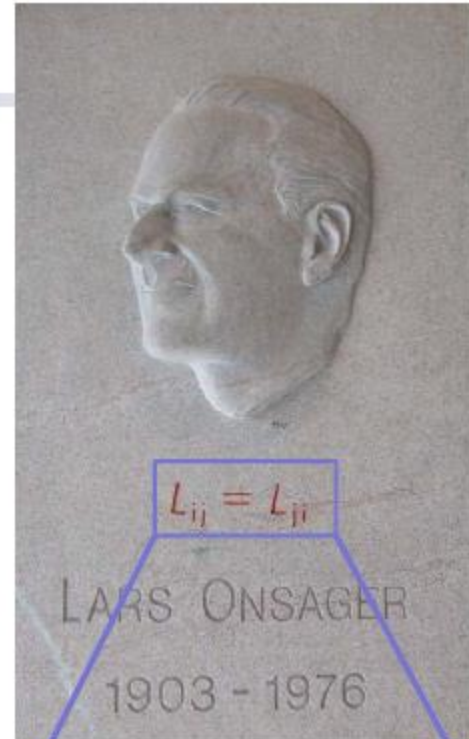
$$\left\{ \begin{array}{l} X_i \\ J_i \end{array} \right. \quad \begin{array}{l} \text{generalized forces} \\ \text{generalized currents} \end{array}$$

$$J_i = \sum_j L_{ij} X_j \quad \text{linear response}$$

$i = \{\text{mass, charge, spin, energy, ...}\}$

$$\dot{S} = \sum_i X_i J_i \quad \text{entropy creation rate}$$

$$L_{ij}(\mathbf{m}, \mathbf{H}_{ext}) = \varepsilon_i \varepsilon_j L_{ji}(-\mathbf{m}, -\mathbf{H}_{ext})$$



Equality between certain relations between flows and forces out of equilibrium

Currents can induce magnetization excitations



A time-dependent magnetization can induce (charge and spin) currents

# Industrial applications

## Read head in hard drives

HDD (Hard Disc Drive)  
Read head

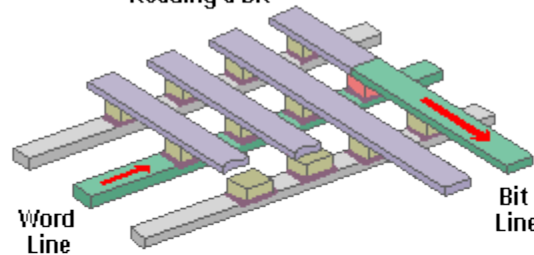


GMR

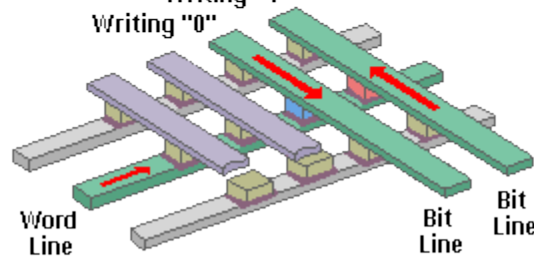


Large TMR + Low R  
Large CPP-GMR

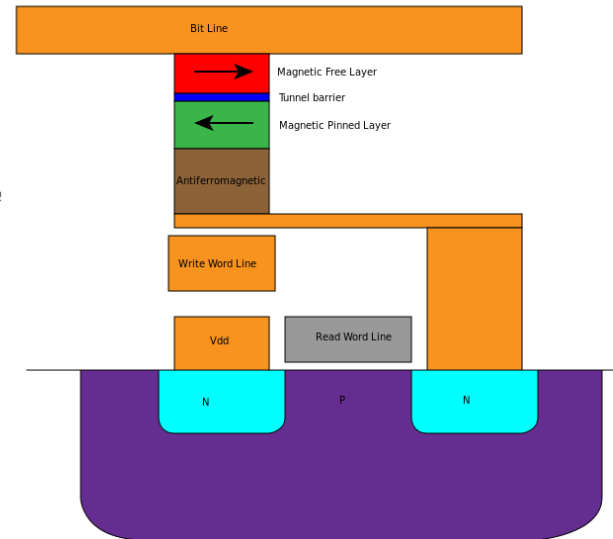
Reading a bit



Writing "1"  
Writing "0"

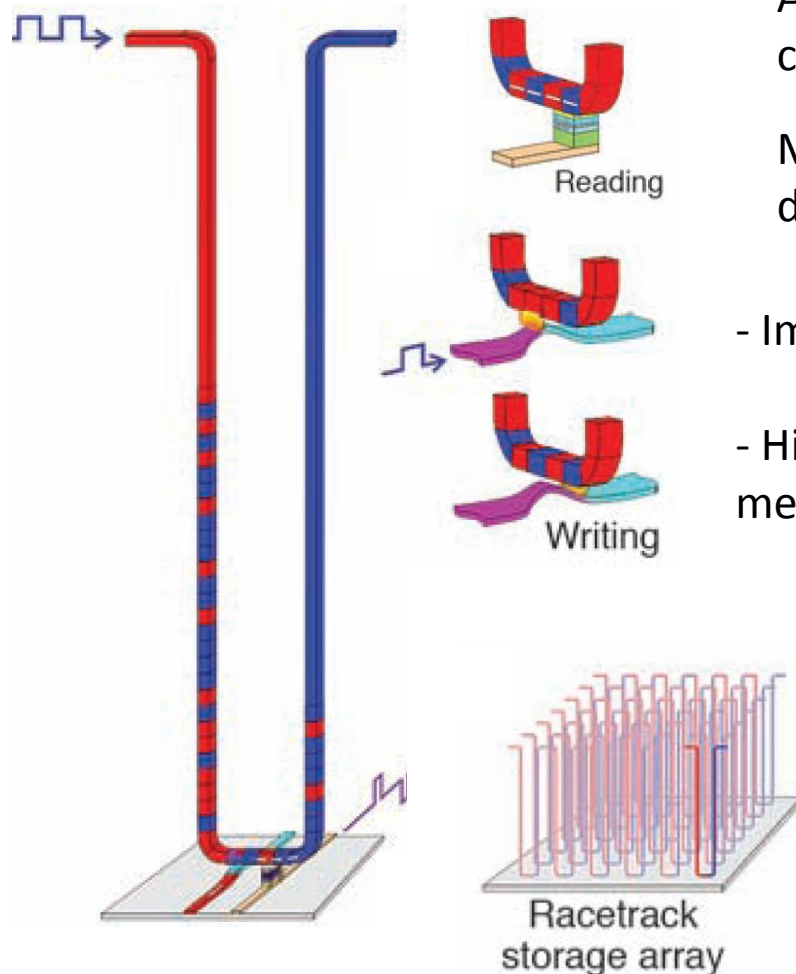


MRAM



# Application of Spin Transfer Torque

## Magnetic Domain-Wall Racetrack Memory



Dr. Stuart S. P. Parkin Science **320**, 190 (2008)

A novel three-dimensional spintronic storage class memory

Magnetic nanowires: information stored in the domain walls

- Immense storage capacity of a hard disk drive
- High reliability and performance of solid state memory (DRAM, FLASH, SRAM...)

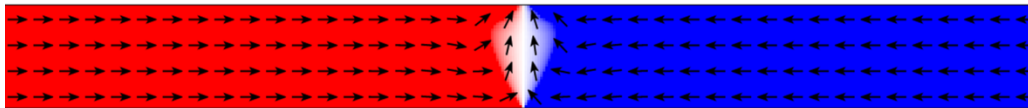
→ **Understanding of current induced domain wall (DW) motion**



# Application of Spin Transfer Torque

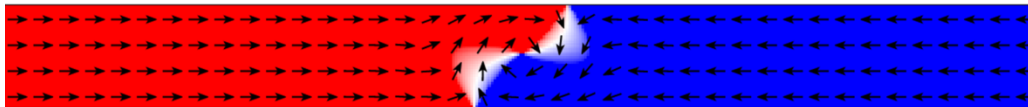
## Domain Wall Structures in Permalloy Nanowires

(a)

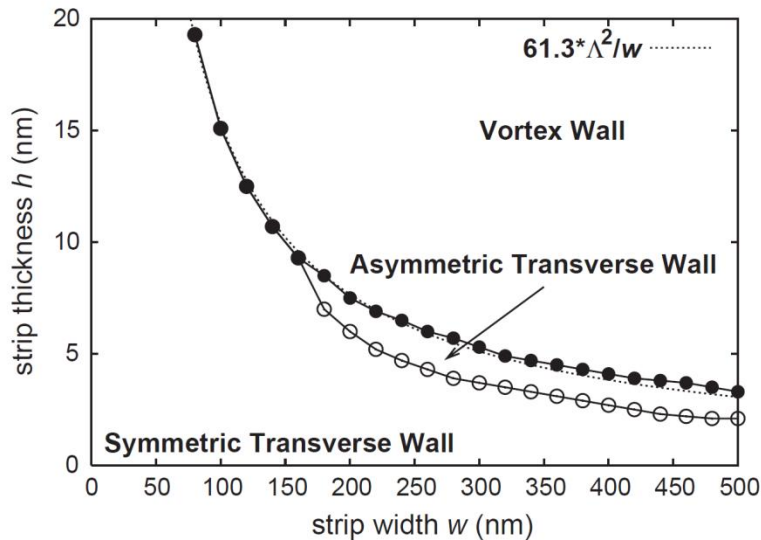


Transvers DW

(b)

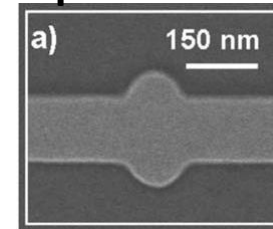


Vortex DW

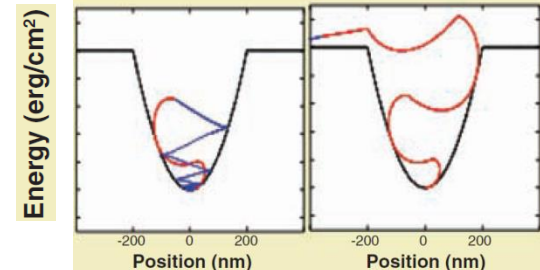
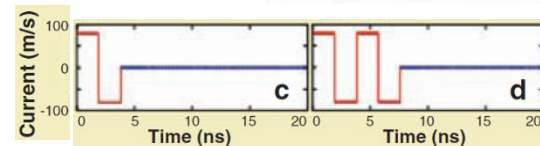
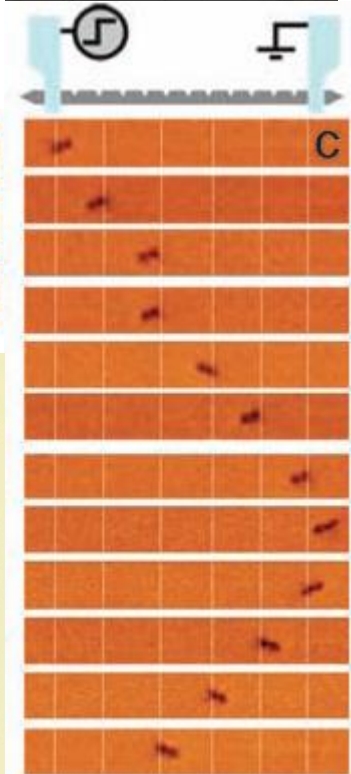
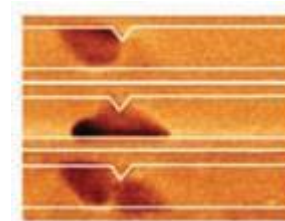
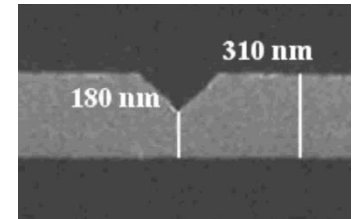


## DW traps

protrusion



notch



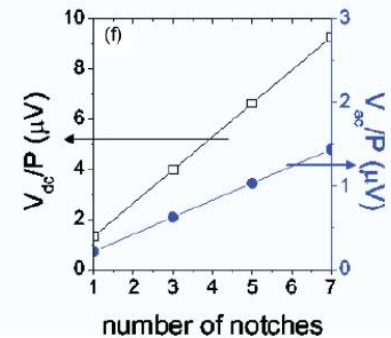
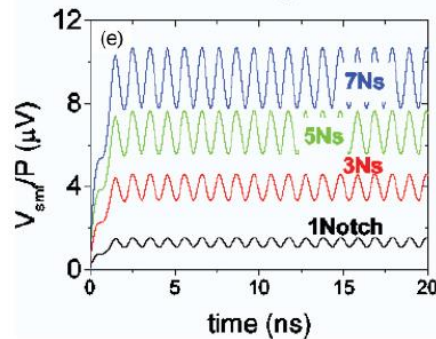
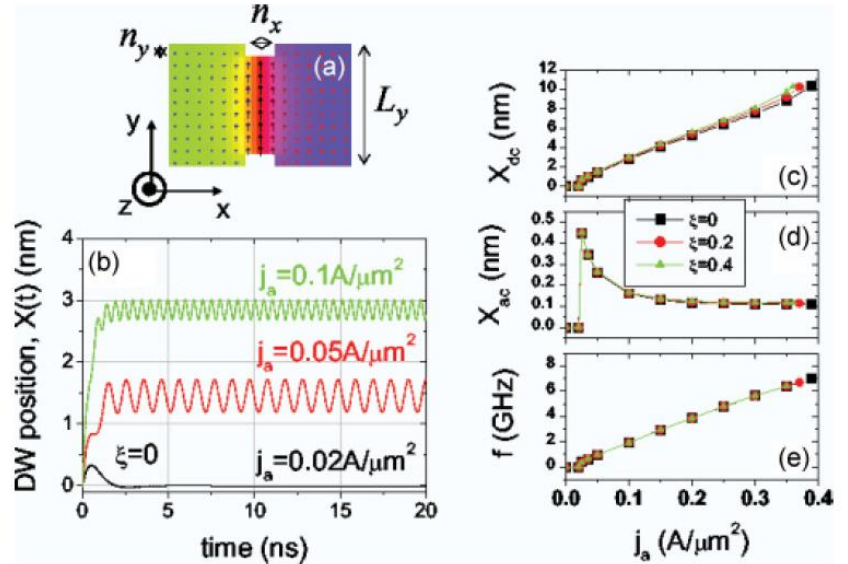
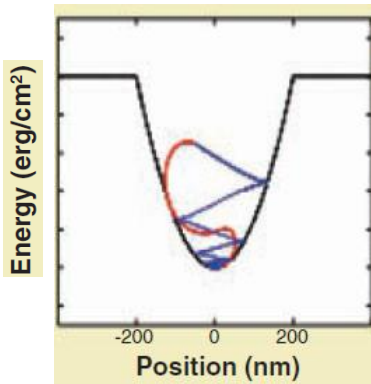
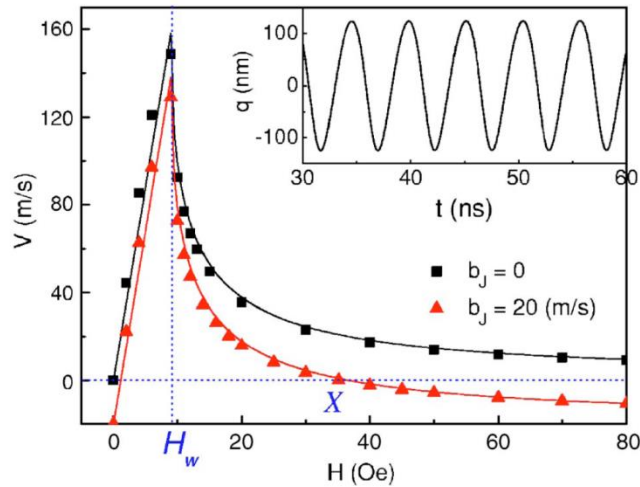
# Application of Spin Transfer Torque

## DW Oscillators

$$j_W < j_a < j_{dep}$$



Walker breakdown

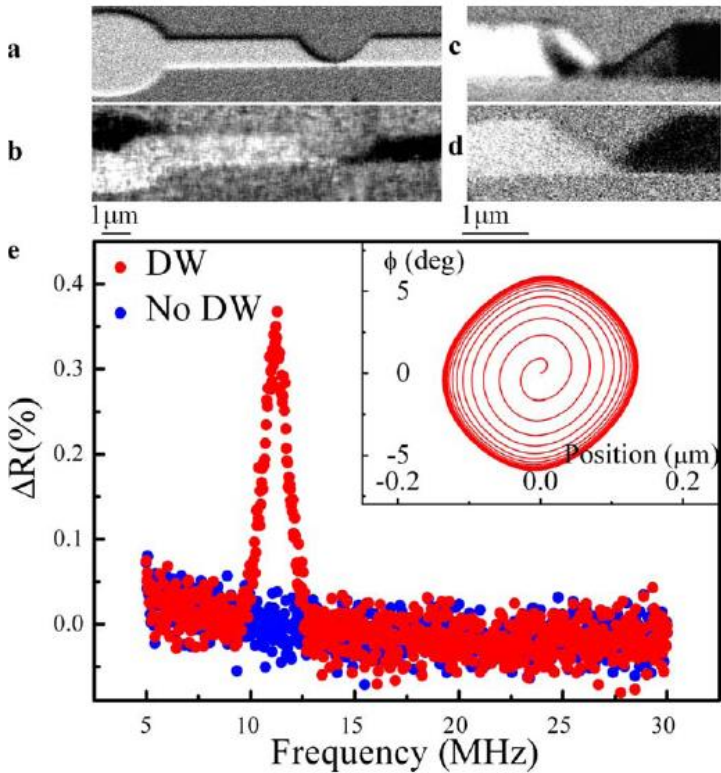


PHYSICAL REVIEW B **83**, 174444 (2011)

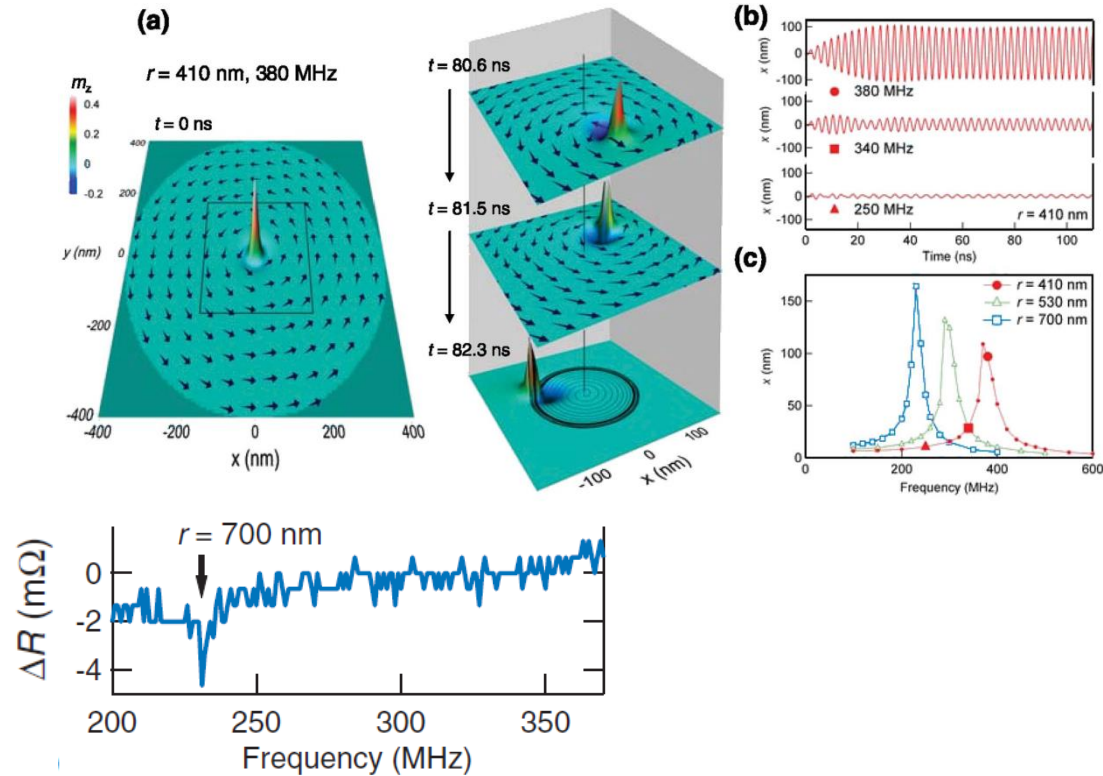
Appl. Phys. Lett. **90**, 142508 (2007)

# Application of Spin Transfer Torque

## AC Current-Induced DW Resonance



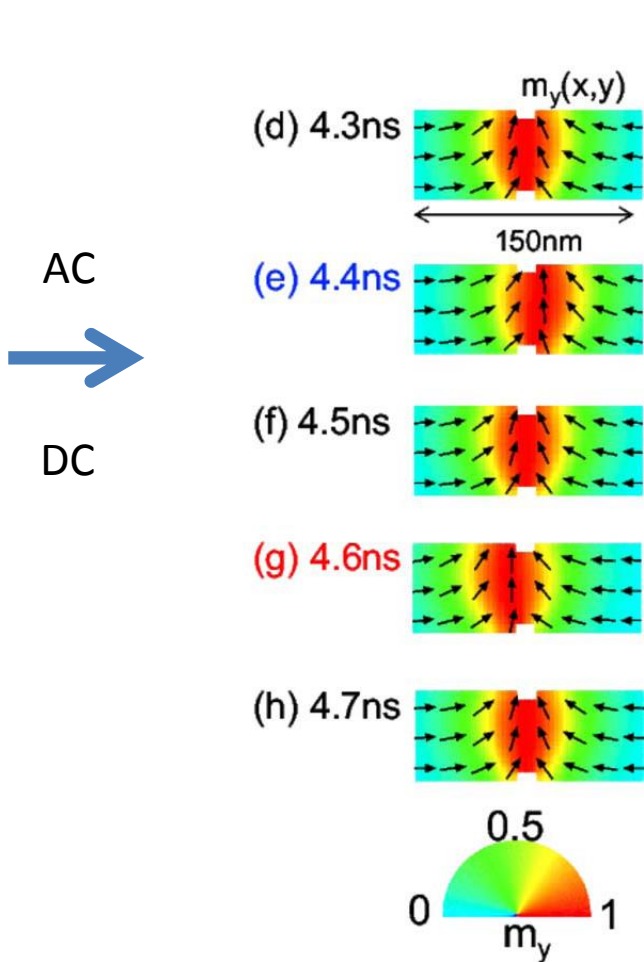
PRB **81**, 060402 (2010),



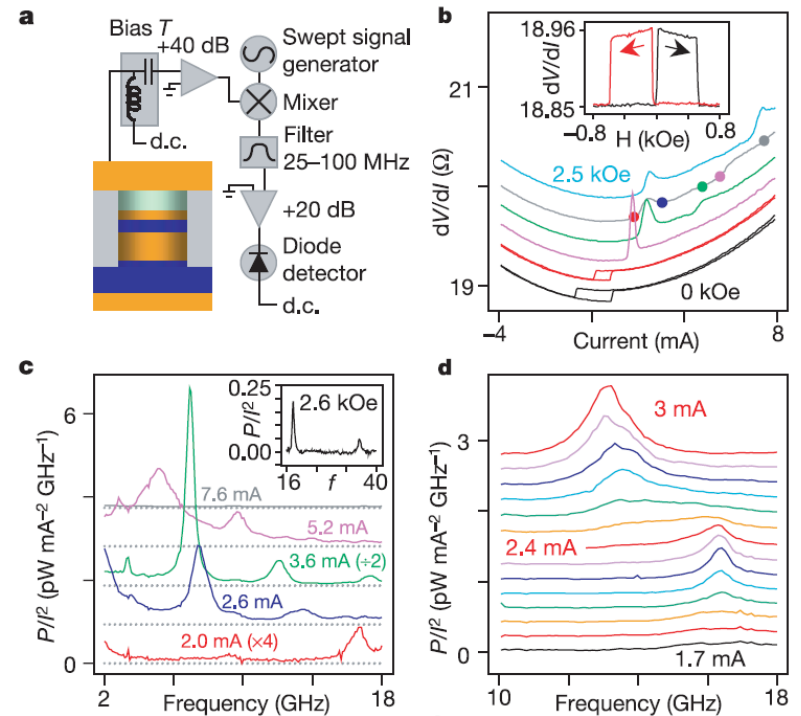
PRL **97**, 107204 (2006)

# Application of Spin Transfer Torque

## Radio-Frequency DW Oscillators



## ✕ CPP-nanopillar

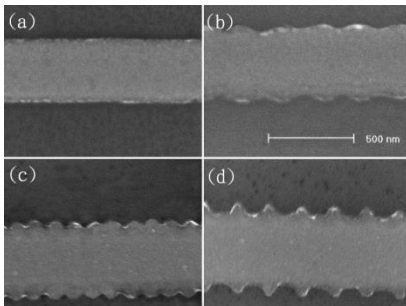
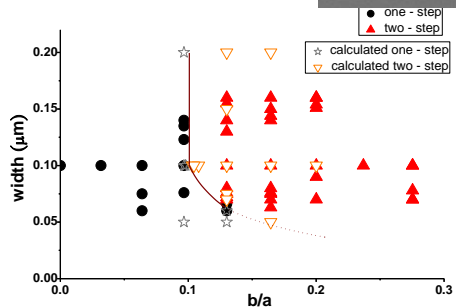


Nature **425**, 380 (2003)



# Our works

## Magnetic nanostructures



- “Quantitative analysis of magnetization reversal in submicron S-patterned structures with narrow constrictions by magnetic force microscopy”. APL **86**, 053111 (2005).
- “Observation of Room Temperature Ferromagnetic Behavior in Cluster Free, Co doped HfO<sub>2</sub> Films”. APL **91**, 082504 (2007).
- “Variation of magnetization reversal in pseudo-spin-valve elliptical rings”. APL **94**, 233103 (2009).
- “Compensation between magnetoresistance and switching current in Co/Cu/Co spin valve pillar structure”. APL **96**, 093110 (2010).
- “Exchange bias in spin glass (FeAu)/NiFe thin films”. APL **96**, 162502 (2010).
- “Demonstration of edge roughness effect on the magnetization reversal of spin valve submicron wires”. APL **97**, 022109 (2010).
- “Current induced localized domain wall oscillators in NiFe/Cu/NiFe submicron wires”. APL **101**, 242404 (2012).
- “Inverse spin Hall effect induced by spin pumping into semiconducting ZnO”. APL **104**, 052401 (2014).

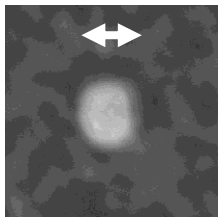
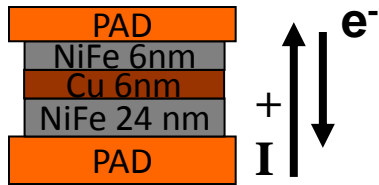
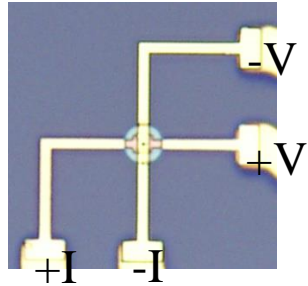
# outline

- Giant Magnetoresistance, Tunneling Magnetoresistance
- Pure Spin current (no net charge current)
  - Spin Hall, Inverse Spin Hall effects
  - Spin Pumping effect
  - Spin Seebeck effect
- Spin Transfer Torque
- **Micro and nano Magnetics**

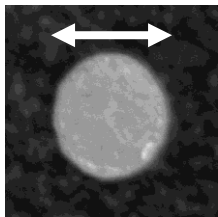
# Nano Magnetism

## Vortex induced by dc current in a circular magnetic spin valve nanopillar

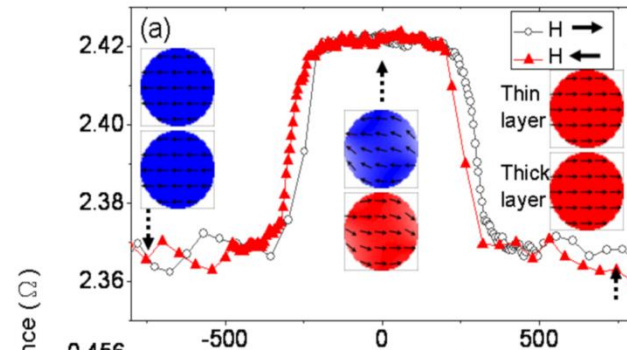
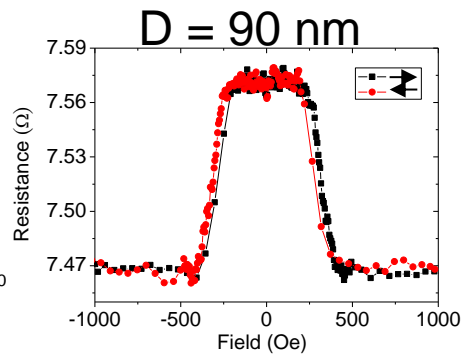
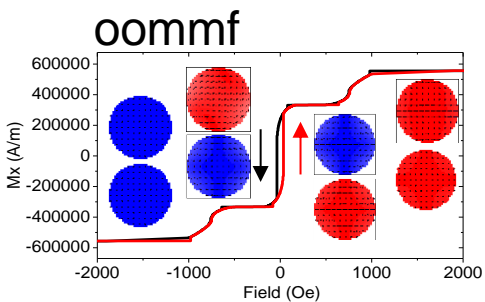
L. J. Chang and S. F. Lee



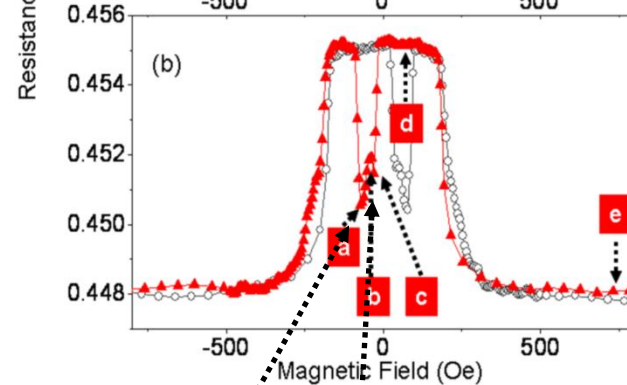
90 nm



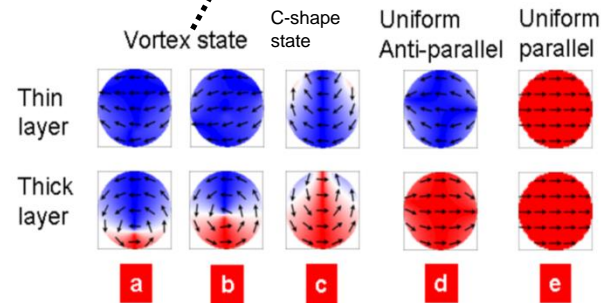
380 nm



D = 160 nm

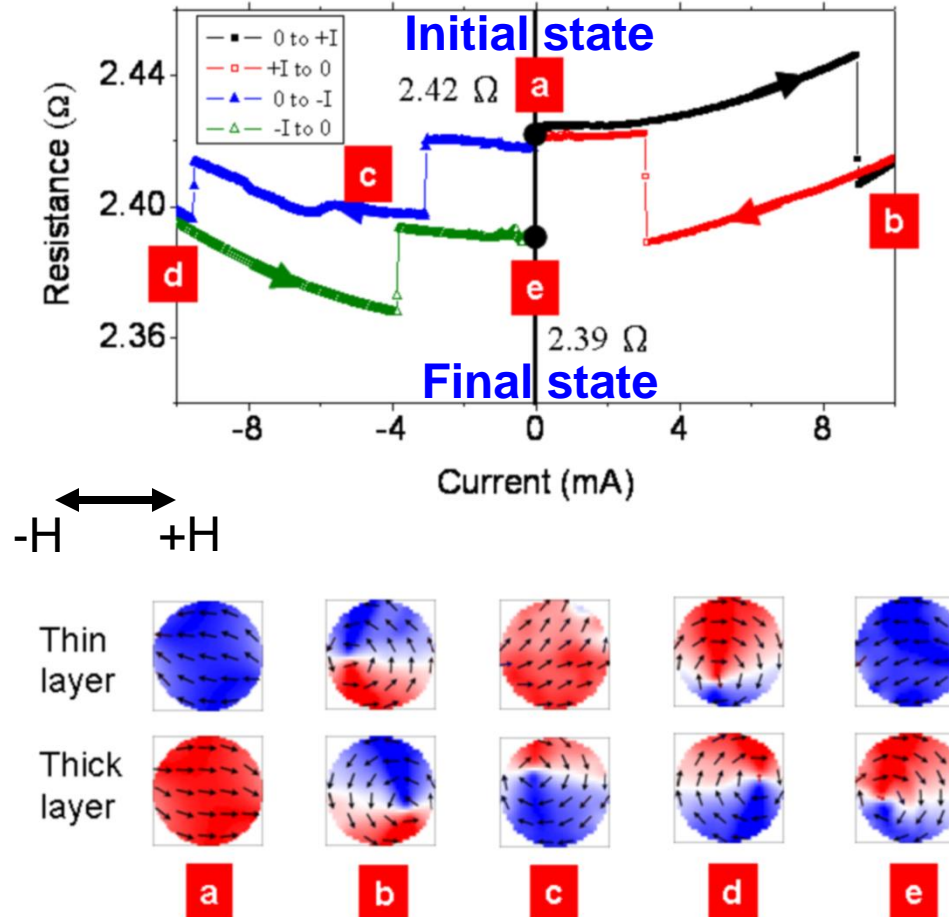


D = 380 nm



# Current driven vortex nucleation

$D = 160 \text{ nm}$     $H = 0 \text{ Oe}$



**Other research interest include superconductor-magnetic material proximity effect, Ferromagnetic Resonance etc.**



# Domain wall oscillation in a trapping potential

## *Theoretical Backgrounds*

### Resonant DW induced by AC spin-polarized current in Ferromagnetic strips

DW dynamics equation

$$(1 + \alpha^2)m \frac{d^2 x}{dt^2} = F_p(x) + F_f + F_s + F_d$$

where  $m = \frac{2(\mu_0 L_y L_z)}{\gamma_0^2 (N_z - N_y) \Delta_0}$  is the effective DW

mass (kg), and the other variables are listed below.

$L_y$  : width of wire (m)

$L_z$  : thickness of wire (m)

$\mu_0$  : permeability ( $4\pi \times 10^{-7} \text{ VsA}^{-1}\text{m}^{-1}$ )

$\gamma_0$  : electron gyromagnetic ratio ( $2.2 \times 10^5 \text{ Vs}^2\text{m}^{-1}\text{kg}^{-1}$ )

$N_z, N_y$  : transverse demagnetizing factors

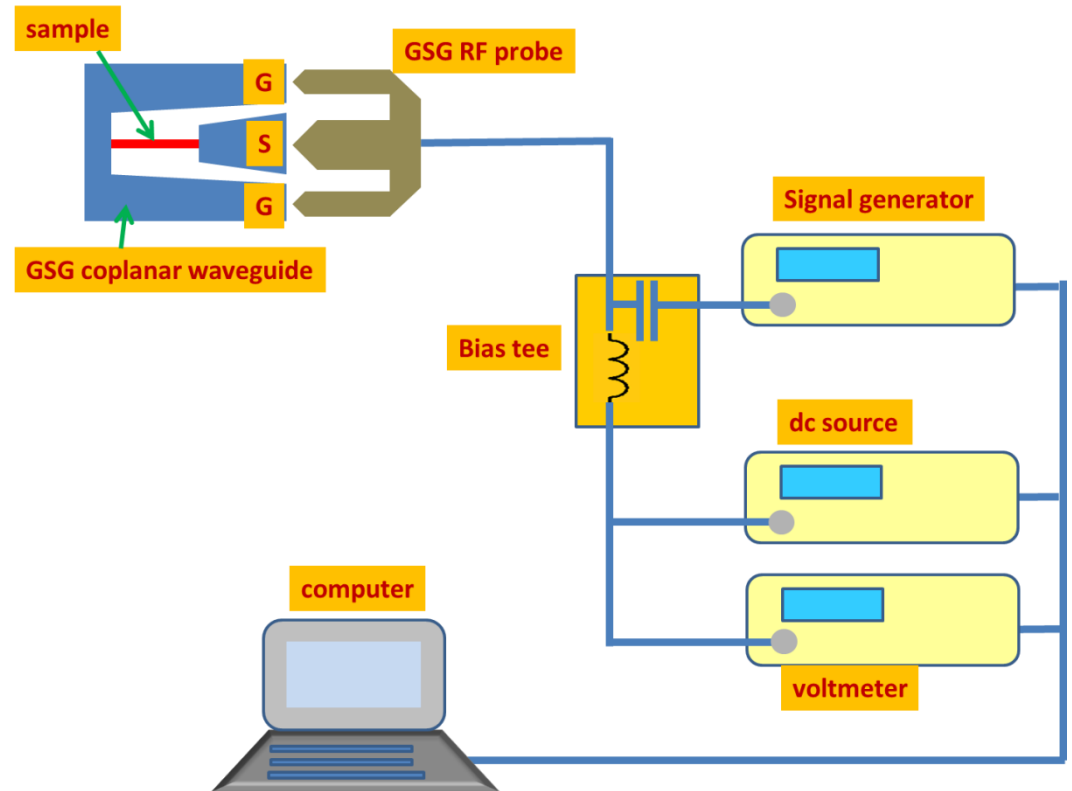
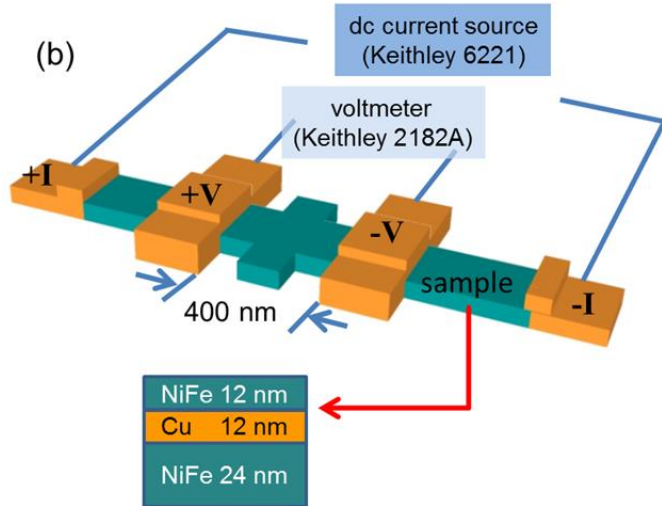
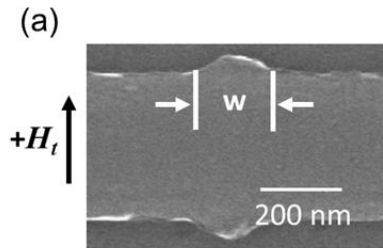
$\Delta_0$  : DW width (m)

$x$  : DW position (m)

# Experiment Methods

## four point probe measurement circuit

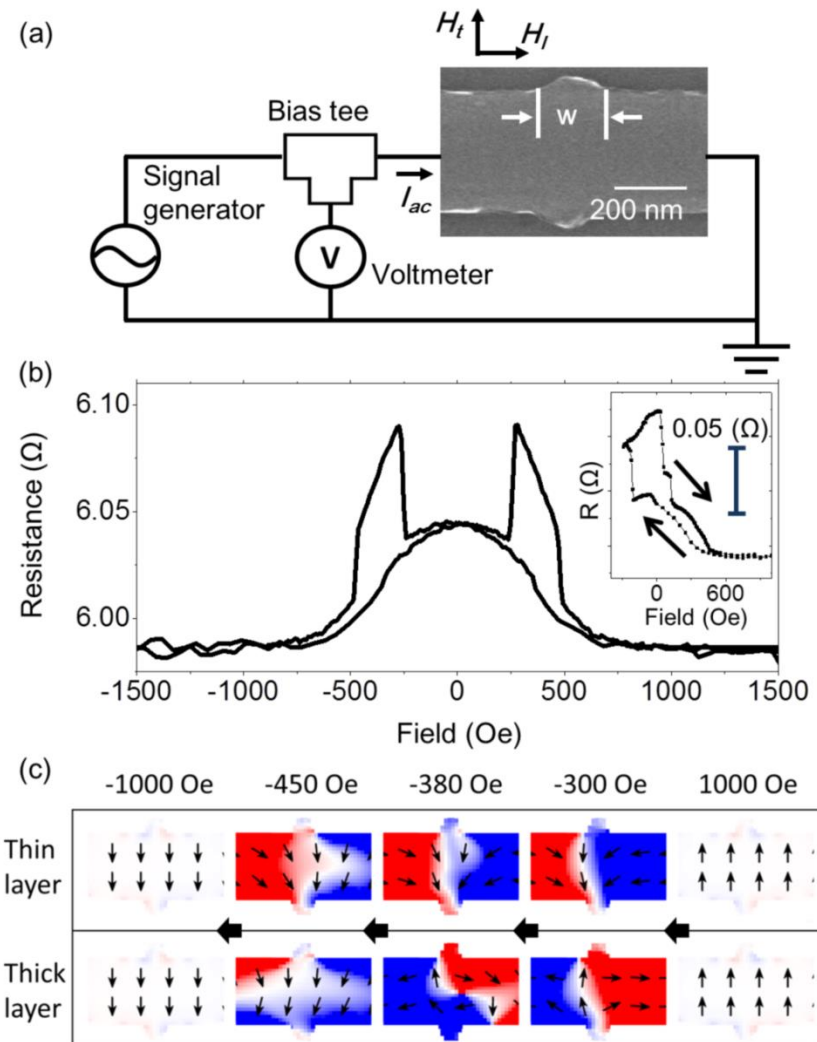
## high frequency measurements circuit



# Measurement and simulation results

## AC current induced localized domain wall oscillators in NiFe/Cu/NiFe submicron wires

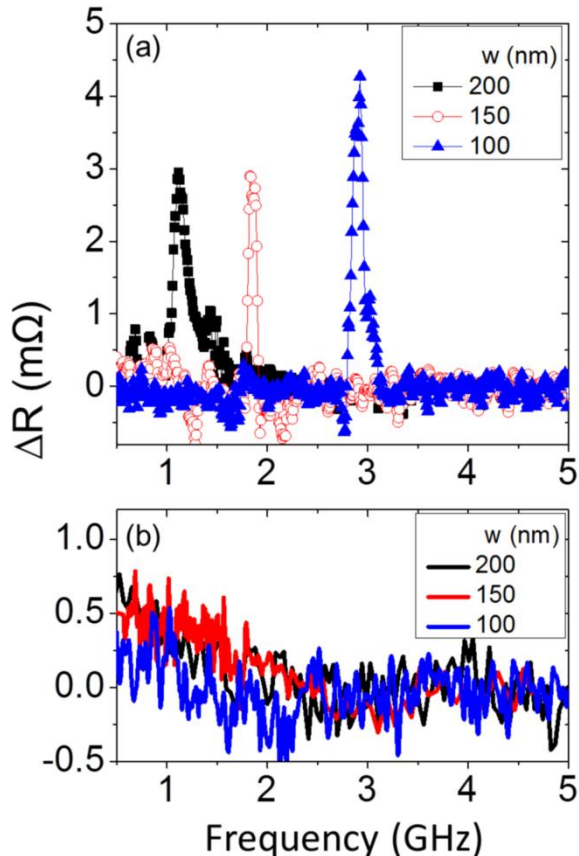
### Nucleation of Pinned anti-parallel transverse DW



# Measurement and simulation results

## AC current induced localized domain wall oscillators in NiFe/Cu/NiFe submicron wires

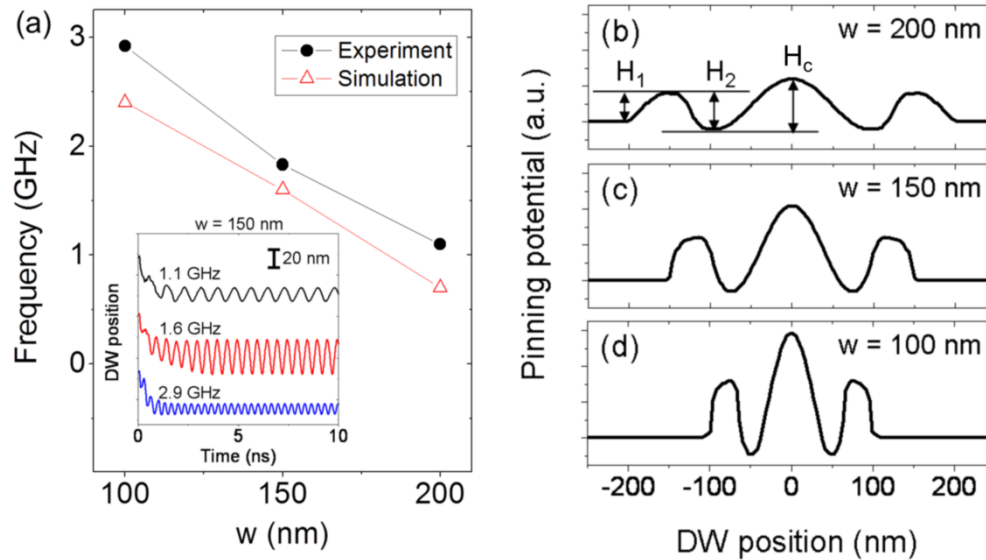
### DW resonators for frequency-selective operation



(a) Experimental measurement of the ac current induces resonance excitation of pinned DW trapped at the protrusion. Resistance change as a function of ac excitation current frequency for the submicron wires containing artificial symmetric protrusions with three different widths of protrusion  $w = 200, 150,$  and  $100$  nm. (b) The response curve measured at the saturation field with a uniform state of submicron wires (without DW). The  $\Delta R$  is observed unchanged with frequency for each of the samples.

# Measurement and simulation results

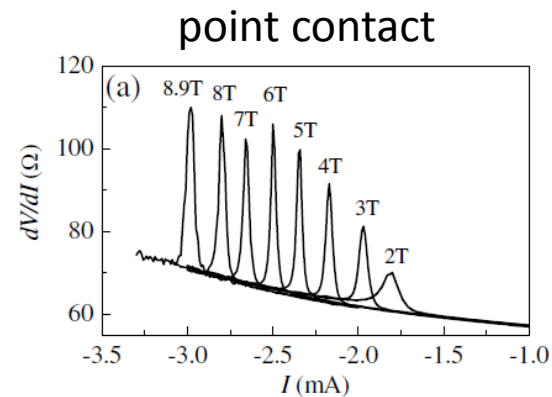
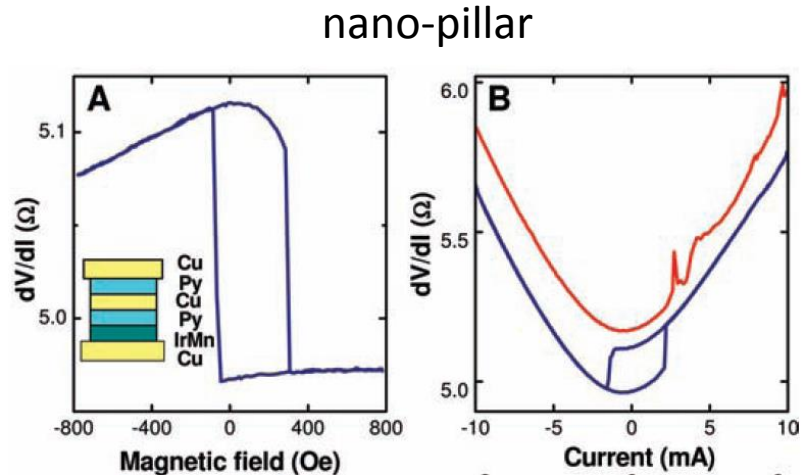
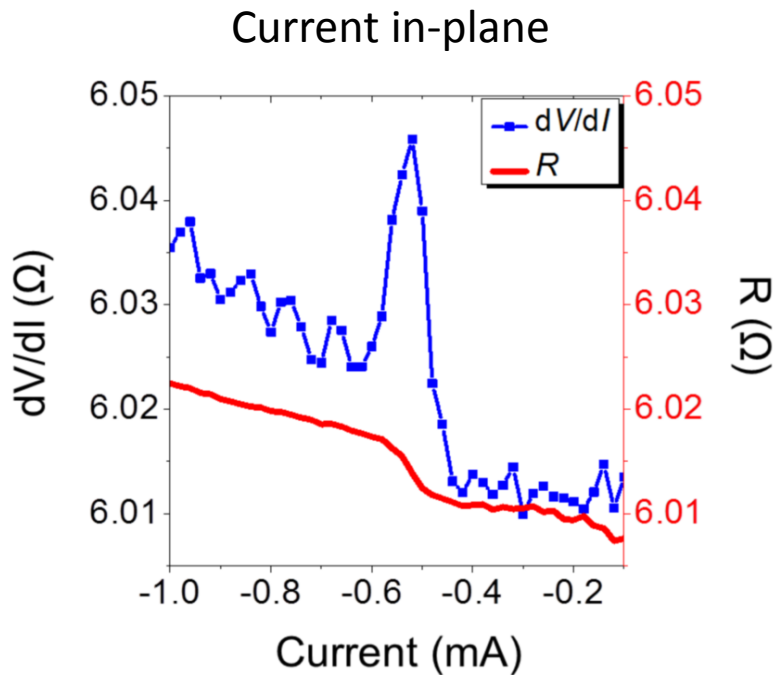
## AC current induced localized domain wall oscillators in NiFe/Cu/NiFe submicron wires



Resonance frequency of pinned DW dependence on the width of trap  $w$ , the solid circles and the open triangles indicate the experiment and simulation results respectively. The inset shows the simulated time evolutions of the DW motion with  $w = 150$  nm. (b)-(d) Potential landscape of pinned DW from micromagnetic simulation with three different width of protrusion  $w = 200, 150, 100$  nm.

# Measurement and simulation results

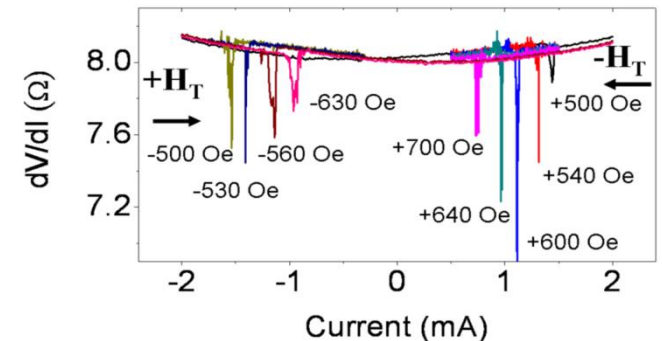
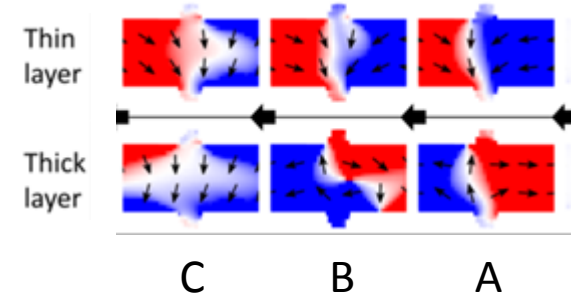
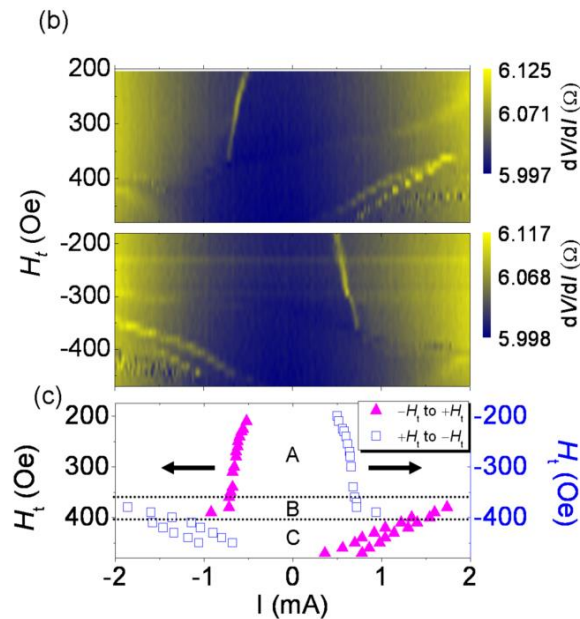
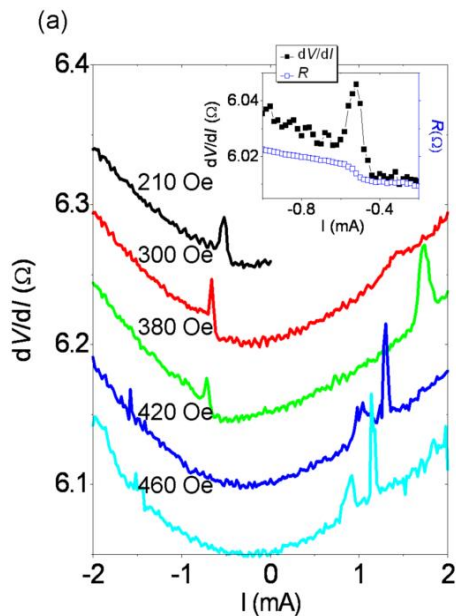
## Reversible domain wall motion induced by dc current in NiFe/Cu/NiFe submicron wires



*Science* **307**, 228 (2005)  
PRL **97**, 107204 (2006)

# Measurement and simulation results

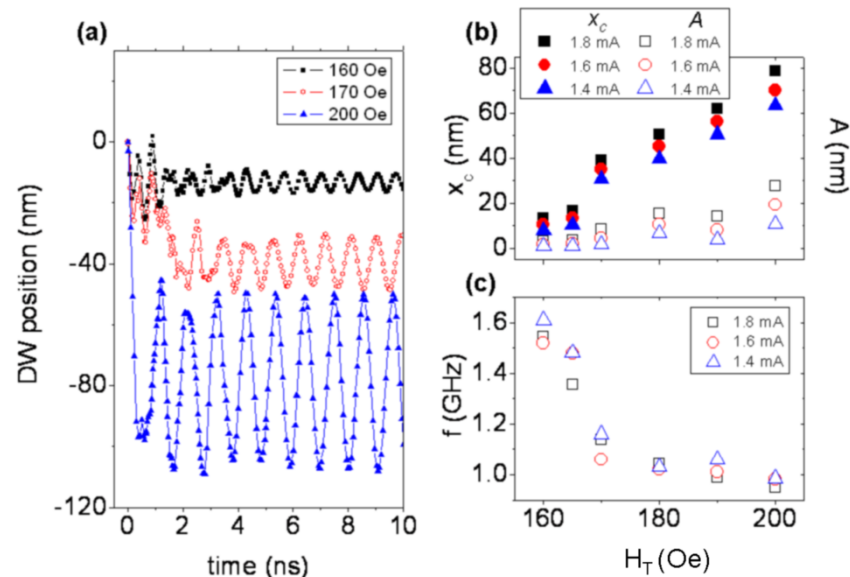
## Reversible domain wall motion induced by dc current in NiFe/Cu/NiFe submicron wires



Differential resistance vs. current density at different external transverse fields  $H_t$ , enlarged in the inset for  $V/I$  vs.  $j$  at  $H_t = 210$  Oe. (b) Map of  $dV/dI$  versus transverse field and dc current. (c) Critical current  $I_c$  vs.  $H_t$ .

# Measurement and simulation results

## Reversible domain wall motion induced by dc current in NiFe/Cu/NiFe submicron wires



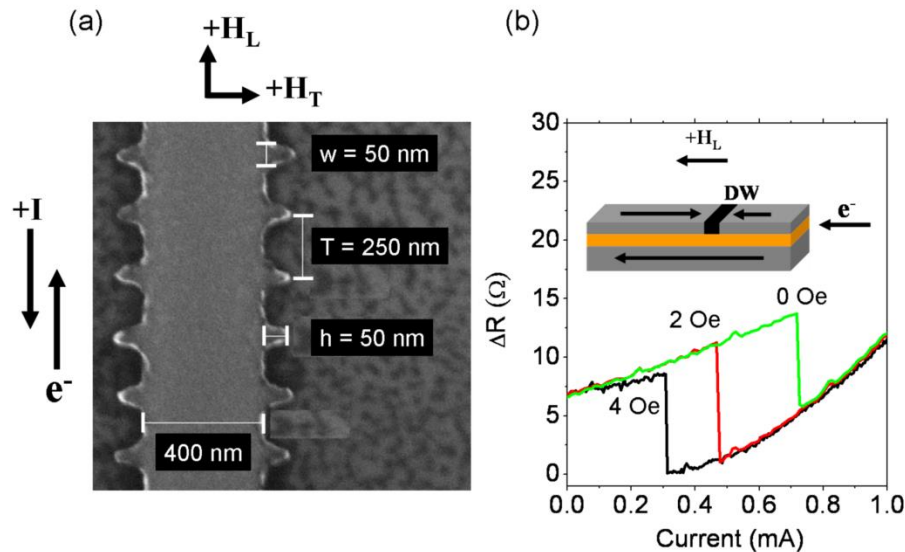
Simulation results of DW position as a function of time under fixed dc current density of  $9.7 \times 10^6$  A/cm<sup>2</sup> with variation of external transverse field  $H_T$ . (b) central position  $x_c$ , amplitude  $A$ , and (c) frequency of the oscillator vs.  $H_T$  with different dc current.



# Measurement and simulation results

## Reversible domain wall motion induced by dc current in NiFe/Cu/NiFe submicron wires

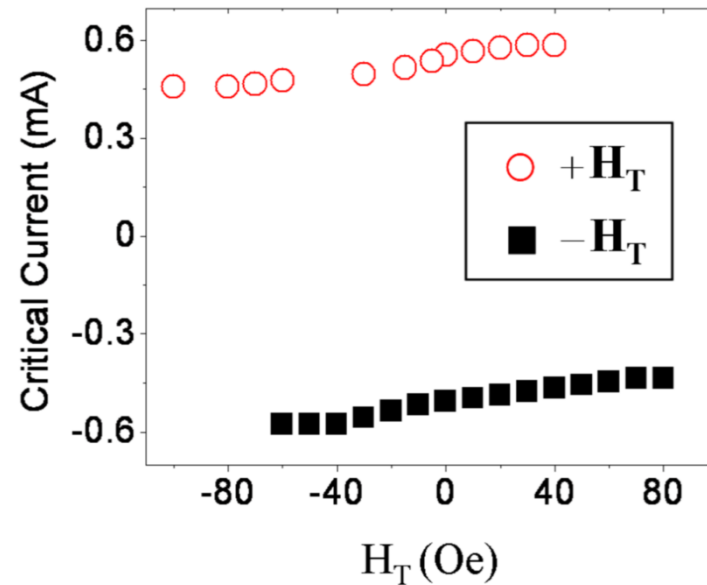
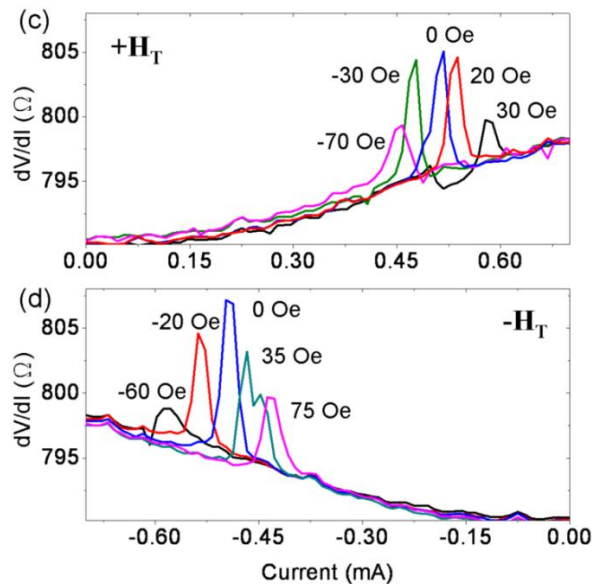
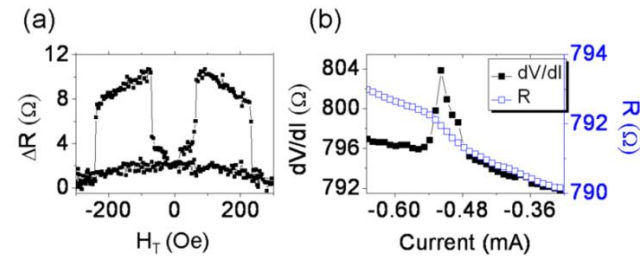
Series of submicron wires with serial DW traps of artificial symmetric protrusions

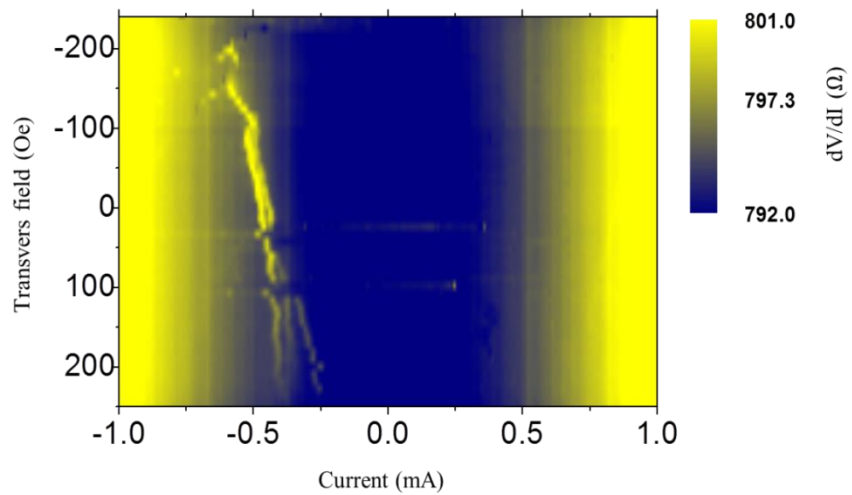
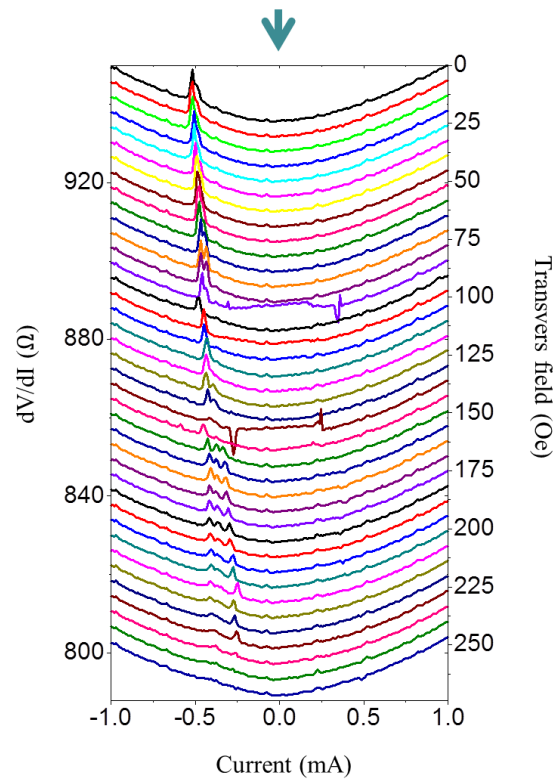
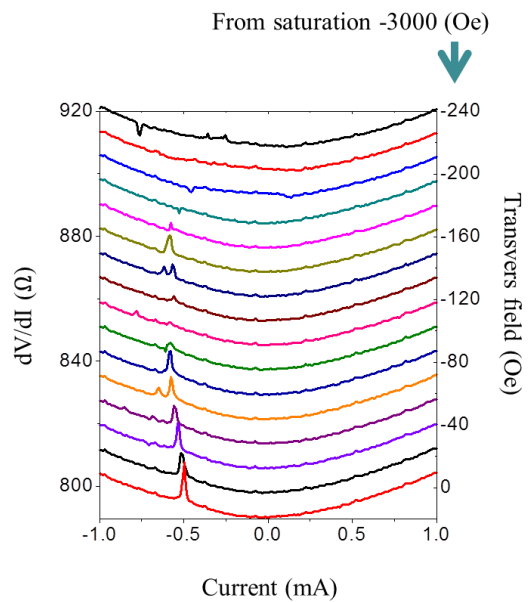


A Scanning electron microscope image of a typical serial-DW-trap sample with the protrusions 50 nm in width and height. The period was 250 nm on either side of the wire. Magnetic field and current directions are specified. (b) Schematic diagram of the sample and the irreversible resistance change from anti-parallel state to parallel state for  $H_L = 0$  (green solid line), 2 (red dash line), and 4 (black dotted line) Oe.

# Measurement and simulation results

## Reversible domain wall motion induced by dc current in NiFe/Cu/NiFe submicron wires





## Summary

- DW oscillation with resonance frequency as high as 2.92 GHz and the resonance frequency can be tuned by the width of protrusion.
- The higher resonance frequency for the narrow trap is due to the steeper potential landscape which enhances the restoring force on the pinned DW.
- For the domain wall oscillations induced by injection of a dc current investigated, the observed peak in  $dV/dI$  associated with the reversible change of magnetoresistance is attributed to the reversible motion of the DW.

# outline

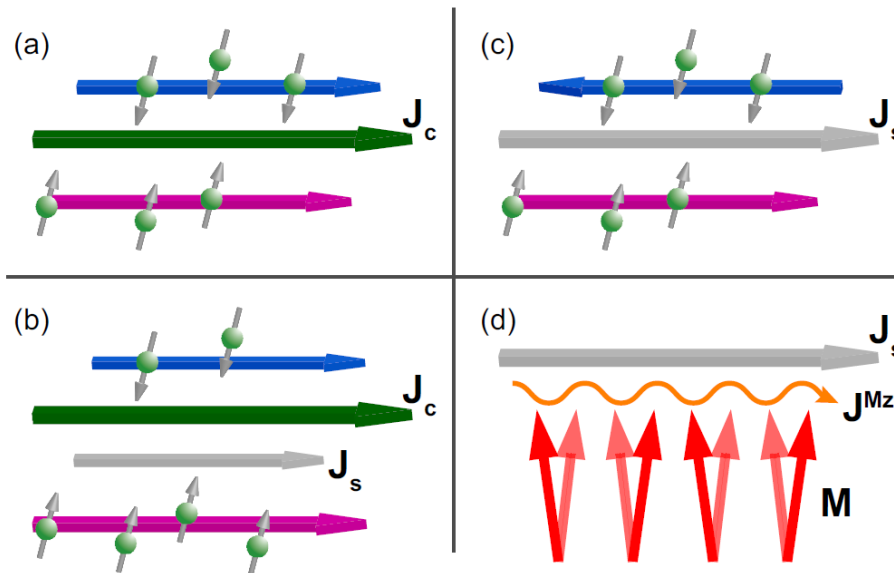
- Giant Magnetoresistance, Tunneling Magnetoresistance
- Spin Transfer Torque
- Pure Spin current (no net charge current)
  - Spin Hall, Inverse Spin Hall effects
  - Spin Pumping effect
  - Spin Seebeck effect
- Micro and nano Magnetics

Spin polarized current vs pure spin current

# Pure Spin Current

-- with no accompanying net charge current

- Theoretically
  - $J_S = \hat{s} \cdot \vec{v} \rightarrow J_S = \frac{d}{dt} (\hat{s} \cdot \vec{r})$
- Experimentally
  - Spin Hall, Inverse Spin Hall effects
  - Spin Pumping effect
  - Spin Seebeck effect



# Spin Current

## Proper Definition of Spin Current in Spin-Orbit Coupled Systems

Junren Shi,<sup>1,2</sup> Ping Zhang,<sup>2,3</sup> Di Xiao,<sup>2</sup> and Qian Niu<sup>2</sup>

<sup>1</sup>*Institute of Physics and ICQS, Chinese Academy of Sciences, Beijing 100080, People's Republic of China*

<sup>2</sup>*Department of Physics, The University of Texas at Austin, Austin, Texas 78712, USA*

<sup>3</sup>*Institute of Applied Physics and Computational Mathematics, Beijing 100088, People's Republic of China*

(Received 19 April 2005; revised manuscript received 18 November 2005; published 24 February 2006)

The conventional definition of spin current is incomplete and unphysical in describing spin transport in systems with spin-orbit coupling. A proper and measurable spin current is established in this study, which fits well into the standard framework of near-equilibrium transport theory and has the desirable property to vanish in insulators with localized orbitals. Experimental implications of our theory are discussed.

$$J_S = \hat{s} \cdot \vec{v} \quad \rightarrow \quad J_S = \frac{d}{dt} (\hat{s} \cdot \vec{r}) = \hat{s} \cdot \vec{v} + \frac{d}{dt} \hat{s} \cdot \vec{r}$$

torque dipole term

1. spin current is not conserved
2. can even be finite in insulators with localized eigenstates only
3. not in conjugation with any mechanical or thermodynamic force, not fitted into the standard near-equilibrium transport theory

1. spin current conserved
2. vanishes identically in insulators with localized orbitals
3. in conjugation with a force given by the gradient of the Zeeman field or spin-dependent chemical potential

# Spin Current

*Advances in Physics*

Vol. 59, No. 3, May–June 2010, 181–255



Taylor & Francis  
Taylor & Francis Group

## Spin currents and spin superfluidity

E.B. Sonin\*

*Racah Institute of Physics, Hebrew University of Jerusalem, Jerusalem 91904, Israel*

*(Received 3 September 2009; final version received 1 February 2010)*

The present review analyses and compares various types of dissipationless spin transport: (1) Superfluid transport, when the spin-current state is a metastable state (a local but not the absolute minimum in the parameter space). (2) Ballistic spin transport, when spin is transported without losses simply because the sources of dissipation are very weak. (3) Equilibrium spin currents, i.e. genuine persistent currents. (4) Spin currents in the spin Hall effect. Since superfluidity is frequently connected with Bose condensation, recent debates about magnon Bose condensation are also reviewed. For any type of spin currents simplest models were chosen for discussion in order to concentrate on concepts rather than the details of numerous models. The various hurdles on the way of using the concept of spin current (absence of the spin-conservation law, ambiguity of spin current definition, etc.) were analysed. The final conclusion is that the spin-current concept can be developed in a fully consistent manner, and is a useful language for the description of various phenomena in spin dynamics.



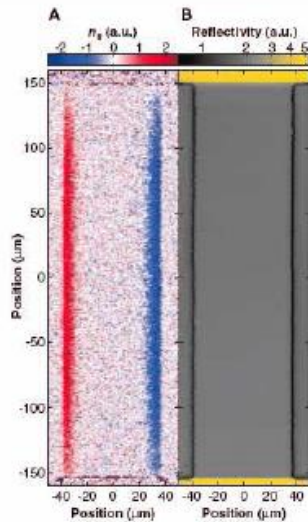
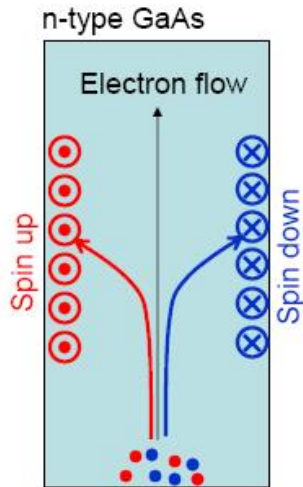
#### 4. Conclusions

The present review focused on four types of dissipationless spin transport: (1) superfluid transport, when the spin-current state is a metastable state (a local but not the absolute minimum in the parameter space); (2) Ballistic spin transport, when spin is transported without losses simply because the sources of dissipation are very weak; (3) equilibrium spin currents, i.e. genuine persistent currents and (4) spin currents in the spin Hall effect. The dissipationless spin transport was a matter of debate for decades, though sometimes they were to some extent semantic. Therefore, it was important to analyse what physical phenomenon was hidden under this or that name remembering that any choice of terminology is inevitably subjective and is a matter of taste and convention. The various hurdles on the way of using the concept of spin current (absence of the spin-conservation law, ambiguity of spin current definition, etc.) were analysed. **The final conclusion is that the spin-current concept can be developed in a fully consistent manner, though this is not an obligatory language of description: spin currents are equivalent to deformations of the spin structure, and one may describe the spin transport also in terms of deformations and spin stiffness.**

The recent revival of interest to spin transport is motivated by the emerging of spintronics and high expectations of new applications based on spin manipulation. This is far beyond the scope of the present review, but hopefully the review could justify using of the spin-current language in numerous investigations of spin-dynamics problems, an important example of which is the spin Hall effect.

# Spin Hall effect

Spin Hall Effect: Electron flow generates transverse spin current



SHE observed in GaAs using Kerr effect to measure spin

Kato et.al. (Awschalom), Science 306, 1910 (2004)

M. I. Dyakonov and V. I. Perel, *JETP* **13** 467 (1971)

J. E. Hirsch, *Phys. Rev. Lett.* **83** 1834 (1999)

Guo *et al*, PRL **100** 096401 (2008)

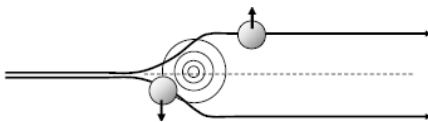
Now observed at room temperature in ZnSe

The **Intrinsic SHE** is due to topological band structures

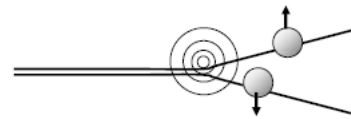
$$\dot{\vec{r}} = \frac{1}{\hbar} \frac{\partial \epsilon_n(\vec{k})}{\partial \vec{k}} + \frac{e}{\hbar} \vec{E} \times \vec{\Omega}(\vec{k})$$

Berry curvature

The **extrinsic SHE** is due to asymmetry in electron scattering for up and down spins. – spin dependent probability difference in the electron trajectories



Side jump



Skew scattering

# Inverse Spin Hall effect

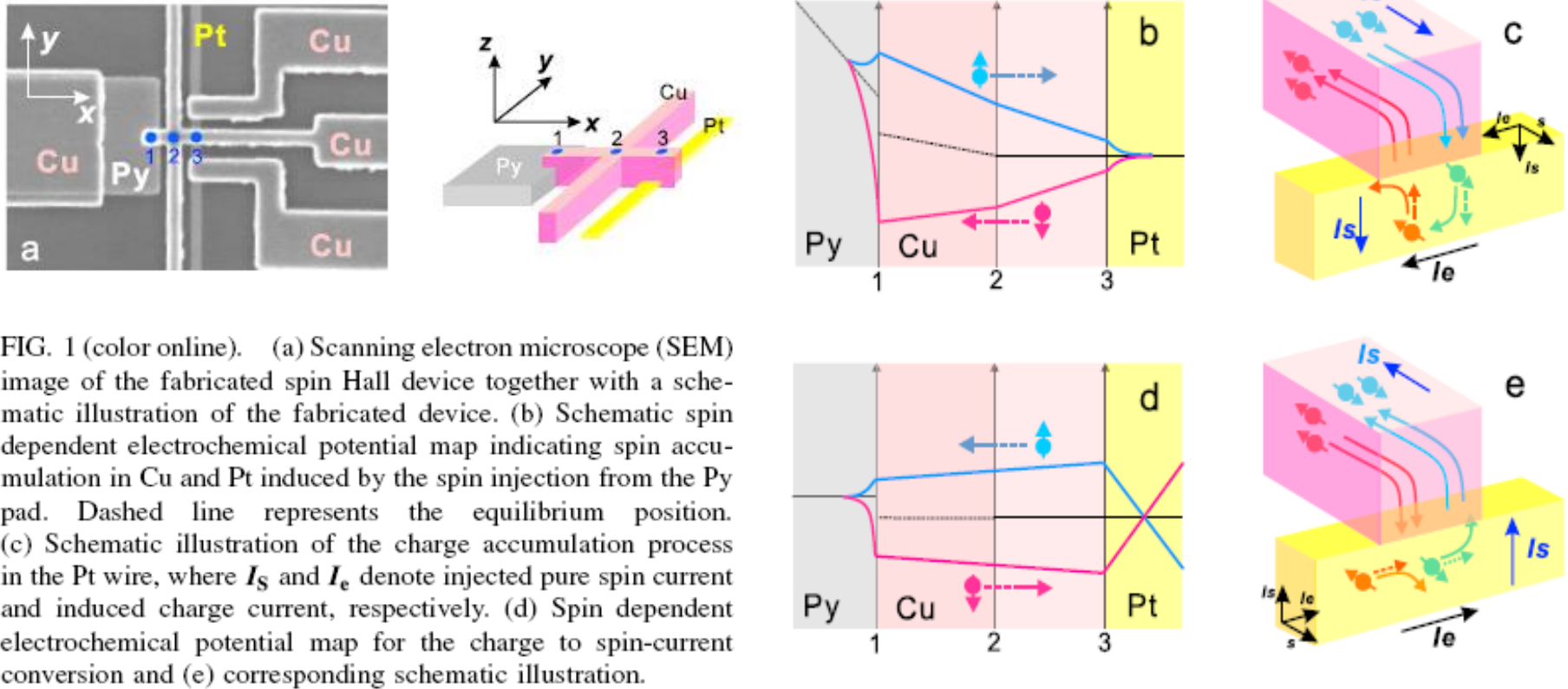


FIG. 1 (color online). (a) Scanning electron microscope (SEM) image of the fabricated spin Hall device together with a schematic illustration of the fabricated device. (b) Schematic spin dependent electrochemical potential map indicating spin accumulation in Cu and Pt induced by the spin injection from the Py pad. Dashed line represents the equilibrium position. (c) Schematic illustration of the charge accumulation process in the Pt wire, where  $I_S$  and  $I_e$  denote injected pure spin current and induced charge current, respectively. (d) Spin dependent electrochemical potential map for the charge to spin-current conversion and (e) corresponding schematic illustration.

Kimura *et al*, PRL **98**, 156601 (2007)

Guo *et al*, PRL **100** 096401 (2008)

# Inverse Spin Hall effect : ISHE

VOLUME 83, NUMBER 9

PHYSICAL REVIEW LETTERS

30 AUGUST 1999

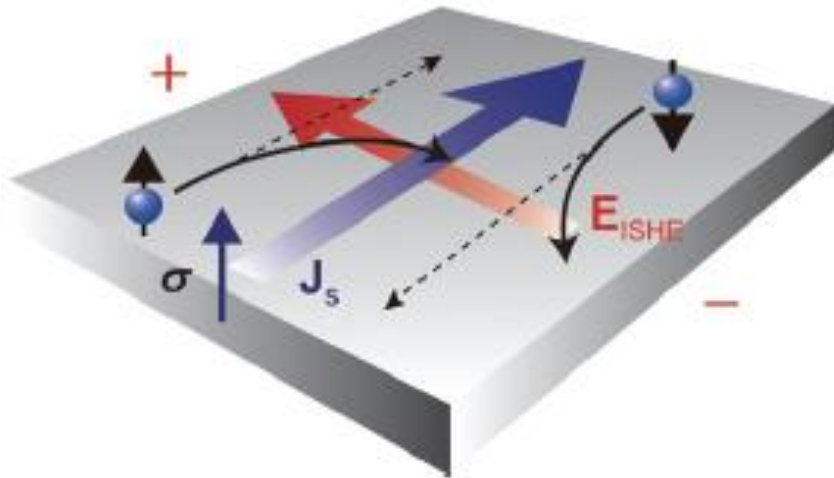
## Spin Hall Effect

J. E. Hirsch

*Department of Physics, University of California, San Diego, La Jolla, California 92093-0319*

(Received 24 February 1999)

It is proposed that when a charge current circulates in a paramagnetic metal a transverse spin imbalance will be generated, giving rise to a "spin Hall voltage." Similarly, it is proposed that when a spin current circulates a transverse charge imbalance will be generated, giving rise to a Hall voltage, in the absence of charge current and magnetic field. Based on these principles we propose an experiment to generate and detect a spin current in a paramagnetic metal.



J. Appl. Phys. **109**, 103913 (2011)

ISHE: converts a spin current  
into an electric voltage

SO-coupling bends the two  
electrons in the same direction →  
charge accumulation →  $E_{\text{ISHE}}$ .

$$\mathbf{E}_{\text{ISHE}} \propto \mathbf{J}_s \times \boldsymbol{\sigma}$$

$\mathbf{J}_s$  : spin current density

$\boldsymbol{\sigma}$  : direction of the spin-polarization vector  
of a spin current.

ISHE: Governed by spin-orbit coupling

# SHE vs. ISHE

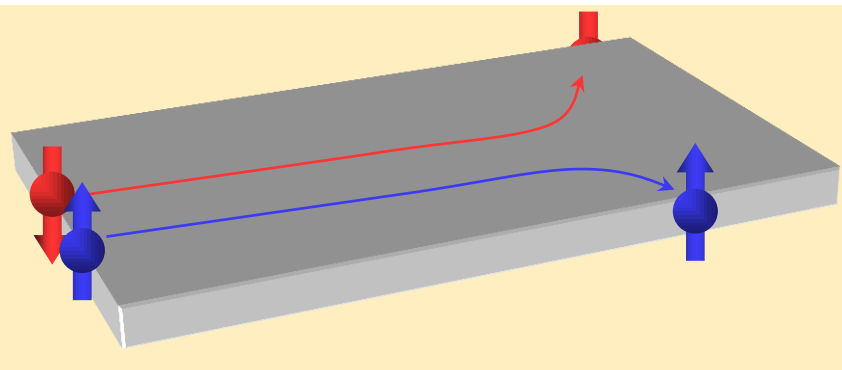
**Spin Hall**

**Charge Current**



**Transverse**

**Spin Imbalance**



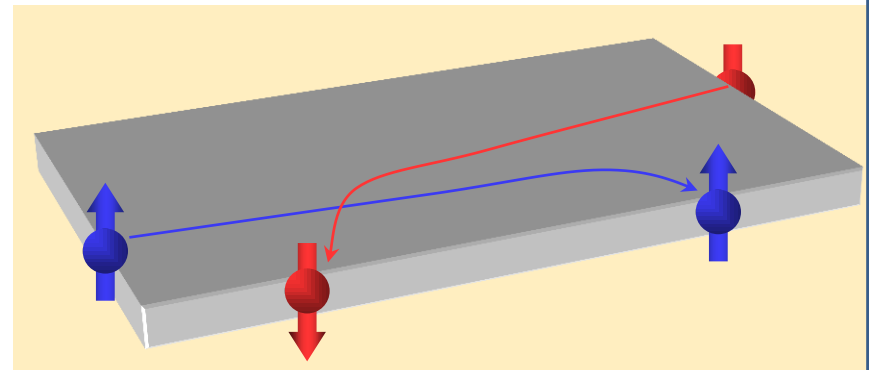
**Inverse Spin Hall**

**Spin Current**



**Transverse**

**Charge Imbalance**



**ISHE : direct & sensitive detection of a spin current !**

# Spin Hall Angle

$$\gamma = \frac{\sigma_{SH}}{\sigma_c}$$

← spin Hall conductivity

← charge conductivity

stronger spin orbit interaction  $\longrightarrow$  larger  $\gamma$